UNIVERSITÀ DEGLI STUDI DI TRENTO

Department of Civil Environmental and Mechanical Engineering

Master course
Environmental and Landscape Engineering

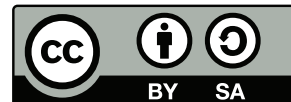Theoretical progress in freezing-thawing processes studies

Advisor
Prof. Riccardo Rigon

Co-advisor
Prof. Stefan Gruber
Dott. Francesco Serafin

Student
Niccolò Tubini

Academic year 2015-2016

CONTACTS

☞ niccolo.tubini@studenti.unitn.it

ACKNOWLEDGEMENTS

> If you want to go fast, go alone
> if you want to go far, go together
>
> —African Proverb

I would first like to thank my thesis supervisor Prof. Riccardo Rigon. He supported me greatly during the last months. Even though I spent three months in Canada he was willing to give me some precious advices. In spite of six hours difference he always found the time for a nice skype call.

I'm grateful to Prof. Stephan Gruber who gave me the chance to join the Permafrost group at Carleton University. His enthusiasm and guidance were really helpful to improve my knowledge of freezing soils.

I would also like to acknowledge Prof. Vincenzo Casulli for the suggestions and nice talks about numerical methods to solve the freezing soils equations.

Finally I express my very profound gratitude to my family and my friends.

CONTENTS

1 | INTRODUCTION

"Hunter-gatherer societies in cold lands have experienced little trouble with perennially frozen ground, and have sometimes used it to advantage, such as for food storage. When gold miners came into Alaska and northern Canada, they learned by trial and error how to thaw permafrost, and the larger mining operators developed fairly sophisticated techniques. Even so, the cost was high, and dealing with frozen ground accounted for half of the cost of mining in the Fairbanks and Nome areas. During past decades, using techniques developed in warmer areas, government agencies and other have erected many buildings in the north only to see them fail because of the thawing of permafrost beneath the foundations. Some home owners have tended to deny the existence of a problem or attributed structural failure to other causes, but most northerners have developed a proper awareness of the hazard of building on ice-rich permafrost and have learned to deal with it. However, people erecting structures on unfrozen soil that overlies permafrost need to realize that foundation problems can developed even if the permafrost table is well below but still within a few tens of meters of the ground surface. Water supply and sewage disposal are critical problems in the continuous permafrost region and a very serious one ever in many areas where the permafrost is discontinuous. Frozen ground limits the availability and quality of water, and it makes sewage and their treatment both difficult and expensive. Another very serious and expensive consequence of seasonally and perennially frozen ground is its effect on transportation facilities–roads, railways, airport runways, and pipelines. Pipelines builders have achieved reasonable success in maintaining pipelines across discontinuous and continuous permafrost areas, but construction and maintenance costs have been high. Less successful are attempts to build surfaces roads that last for more than a few years, and this is an arena in which much needs to be learned [18]."

Permafrost is a product of cold climatic conditions and is widespread in high-latitude and high-elevation environments. A large portion of existing permafrost formed during Pleistocene glacial intervals, and is degrading under contemporary conditions [115].

Permafrost is a key component of the cryosphere through its influence on energy exchanges, hydrological processes, natural hazards and carbon budgets – and hence the global climate system. The climate-permafrost relation has acquired a greater importance with the increasing awareness that rising temperatures, widely expected throughout the next century, may particularly affect permafrost environments [85]. The Intergovernmental Panel on Climate Change (1990) has advocated that research should be directed towards addressing the climate-permafrost relation, including the effects of temperature forcing from climatic variation, local environmental factors such as snow and vegetation, and surficial sediments or bedrock, types. This

was restated by IPCC report of 2013 in which is highlighted that the warming of the climate system is unequivocal, and is now evident from observations of increases in global average air and ocean temperatures, widespread melting of snow ice, and rising global mean sea level. Moreover, permafrost has been identified as one of six cryospheric indicators of global climate change within the international framework of the World Meteorological Organization (WMO) Global Climate Observing System [8].

1.1 MODEL BACKGROUND

Scientific interest in the movement of water trough soil under freezing conditions goes back at least to Buoyoucos (1916) but it is only since 1970s that rigorous theories have been developed to describe heat and mass transfer in freezing porous media [41].

Unlike the other cryospheric phenomena such as glaciers or sea ice, permafrost is a largely invisible phenomenon. Therefore, modeling based on thorough process understanding is the best method for estimating permafrost spatial distribution patterns in the past, present and future [34].

A model is a conceptual or mathematical representation of a phenomenon, usually conceptualized as a system. It provides an idealized framework for logical reasoning, mathematical or computational evaluation as well as hypothesis testing [85]. Each model is based on some hypothesis useful to reduce the complexity of the natural phenomenon and at the same time allow to provide answers to well-posed question [85] [54]. The value of a model depends on its usefulness for a given purpose and not sophistication [85][54].

Permafrost models are a subset of a more general class of geothermal models. In permafrost models, ground freezing and thawing are central in determining the important variables and parameters of which the model is comprised [85]. Existing algorithms to simulate ground thawing and freezing depths vary in the: types of algorithms, parameterizations of soil thermal properties for both frozen and unfrozen soils, parameterizations of unfrozen water content in frozen soil, treatment of latent energy during thawing and freezing, and settings of model configurations such as resolution of time step and soil layers, and the boundary conditions [117].

There are three categories of algorithms to model freezing/thawing ground: empirical and semiempirical, analytical, and numerical.

Empirical and semiempirical algorithms relate freezing and thawing processes to some aspect of surface forcing by one or more experimentally established coefficients [4].

Analytical algorithms are specific solution to heat conduction problems under certain assumptions. The most widely applied analytical solution is Stefan's formulation, which is most applicable in wet homogeneous ground conditions [61].

Numerical algorithms determine the ground thawing and freezing depth by interpolating isothermal positions from the soil temperature profile, which is numerically solved from the heat transfer equation [117]

The analysis of freezing/thawing depths and the ice content in the ground are extremely important for hydrological models. Studies have shown that proper frozen soil schemes help improve land surface and climate model simulations [103] [93]. Given the importance of frozen ground to water and energy cycling near the ground surface, representing the ground thawing and freezing depths in land surface models and hydrological models is critically important [62]. For example, comparison of result from the Project for Intercomparison of Land Surface Parameterization Scheme Phase 2(d) [PILPS 2(d)] have shown that the models with an explicit frozen soil scheme give a much more realistic soil temperature simulation during winter than those without a frozen scheme [62].

However the inclusion of freezing-soil algorithms in hydrological models is challenging, for a series of reasons.

As reported by Kurylyk [54], nowadays there is a lack of a proper fundamental understanding of physical processes involved in freezing-thawing soils.

The thermal and hydraulic properties of frozen soils are distinct from those of the same soil in the unfrozen state [55][79]. The latent heat consumed (released) during thawing (freezing), along with changes in soil thermal properties, greatly alters the surface and subsurface energy partitioning in the soil [81].

In permafrost-dominated watersheds, snowmelt is typically a considerable portion of water inputs [13]. Furthermore snow cover modifies the energy exchange processes between the atmosphere and the ground due to its insulating properties and high albedo [46]. A proper representation of the snow evolution can provide the right time window of direct soil exposure to solar radiation, and, in turn, a reliable quantification of the soil energy fluxes. This is important in regions where the snow cover lasts for many months.

Infiltration and redistribution of meltwater are strongly controlled by soil thawing in the active layer due to the impermeable nature of the frozen soil and the large vertical changes in soil hydraulic conductivity [81]. At the same groundwater flow can enhance permafrost thawing.

Recently, efforts have been made to predict changes in climate forcing with comprehensive numerical models including thaw/freeze algorithms [57][119]. Although climate warming scenarios used by most studies are similar, their predictions differed markedly. Large discrepancies in the predictions of future permafrost fate suggest that further examinations of the basic model assumptions and simulation processes including the thawing and freezing are necessary [12].

Permafrost is a long-term phenomenon and often formed by freezing conditions over hundred of years or millennia. Modeling its evolution at depth is challenging, because phase change and the slow velocity of the temperature signal provide the system with a high thermal inertia. One of the main difficulties lies therefore in the derivation of the initial conditions of the temperature and ice content in the ground. In fact, an unrealistic temperature initialization may take several hundred or thousand of years (of simulated time) to equilibrate with surface conditions. In this case, it becomes difficult to distinguish between real transient effects represented by a model and the

delayed response to an initialization that did not correspond to real conditions [17]. Particular attention needs to be paid to the boundary conditions. The ground surface temperature (i.e., the upper boundary condition) is a key input for all ground thawing and freezing depth algorithms. Although uncertainties in current methods to estimate [44] or simulate [118] surface temperature remains one of the largest sources of error in soil thermal simulations [44]. As a matter of fact, the relationship between mean ground temperatures and mean air temperatures reflects complex interaction between a range of variables including aspect, surface cover, soil moisture status and winter snow depth. [11].

Another difficulty is related to the high topographical heterogeneity. The meteorological forcings may drastically vary in short distances, and represent important parameters that can influence the presence and degradation timing of permafrost [30]. This is one of the main feature that has to be considered in mountain regions. Certain analytical algorithms and all numerical algorithms require a well-defined lower boundary. Although soil temperature measured or simulated at the bottom of soil column could serve as a lower boundary condition [111], typically such inputs are unavailable. A frequently used bottom boundary conditions is a geothermal flux [116], or a zero heat flux [118] at a certain ground depth. However, the placement of lower boundary needs special caution [97] particularly when long term simulation is required.

Since the 1970s many authors proposed different model to study the freezing/thawing ground. However it is worthwhile to clarify that even though these studies started about fifty years ago they are characterized by considerable inconsistencies in both the nomenclature and underlying theories or methodologies [54].

Harlan [33] describes the simultaneous heat and fluid transport in a partially frozen porous medium applying the analogy between liquid transfer in partially frozen soils and that in unsaturated soils. From a mathematical point of view his model solves the mass and energy conservation equations with an implicit finite difference scheme, where the unknowns are temperature and soil water potential. In the mass conservation equation, the change in ice content is taken into account by a source/sink term; in the energy conservation equation the phase change appears in the apparent heat capacity. His results are in good qualitative agreement with both field observations and laboratory observations. The freezing process induces the movement of both heat and mass from warm regions to cold regions. As freezing takes place, the moisture content in the unfrozen soil zone decreases sharply toward the freezing front, water migrating to the cold side.

Fuchs et al. [24] developed a theory of soil freezing applicable to unsaturated conditions with solutes present in the soil. The presence of solutes lowers the melting temperature and hence the relationship between temperature, water content and thermal properties of the soil. Like Harlan's model, the phase change is taken into account by the apparent heat capacity while the heat advected by water flow is modeled by an apparent thermal conductivity. Thus the simultaneous heat and water transport equations resulted in a merged single differential equation for heat.

Jame and Norum [41], pointed out the significant effects that the water flow has on the ground thermal regime comparing the temperature profiles obtained by considering simultaneous heat and mass transfer and assuming that there is no water movement in soils.

McKenzie et al. [66] proposed a coupled groundwater flow and heat transport model for saturated conditions. The major constraint of this model is that the thermal and hydraulic properties of soil are strongly affected by the degree of saturation.

Thomas et al. [99] presented a one-dimensional coupled heat flow, water movement, and mechanical deformation model. The emphasis of these authors was on ice segregation and applications to permafrost related mass movement.

Dall'Amico et al. [16], develop a robust method for solving the energy and mass conservation equations dealing with phase change in variably-saturated soil. The assets of this method are: the energy and mass conservation equations are decoupled and solved using a splitting method; a very robust solution based on the globally convergent Newton scheme is used; the soil freezing curve implies that the ice content depends not only on temperature but also on the total water content, making this scheme usable in non-saturated conditions.

It is worth to underline that in recent years the better comprehension of the inter-relationship between the groundwater flow and the heat flux in the ground has stressed the importance of finding adequate numerical method to solve the coupled system of mass and energy balance equations.

1.2 OVERVIEW OF THE CHAPTERS

The thesis is structured as follows:

CHAPTER 1 *Introduction* illustrates the main features and challenges related to the modeling frozen soils.

CHAPTER 2 *Permafrost* provides an overview about what is permafrost, and briefly outlines the environmental feedback and engineering problems related to the degradation/aggradation permafrost processes.

CHAPTER 3 *Physics and equations of water in soils according to Mualem's conceptualization* illustrates models to characterize the soil moisture content, the relative hydraulic conductivity according with Mualem's model. Besides the empirical-cure-fitting models (e.g. Brooks and Corey, and Van Genuchten) it is presented a retention model proposed by Kosugi which parameters are closely related to soil characteristics. Additionally it is presented the derivation of the equations for mass and energy conservation in unsaturated soil.

CHAPTER 4 *Physics and equations of water in freezing soils* provides a derivation of the thermodynamic equilibrium condition between ice and water in soils, under the *freezing=drying* assumption. The freezing point depression due to the capillary forces and the presence of dissolved solutes is derived following the works by Dall'Amico and Acker. Hence the Kosugi's model is extended to characterize the water and ice content in soils. Finally the equations for mass a the energy for frozen soils are derived.

2 | PERMAFROST

2.1 INTRODUCTION

Water is ubiquitous in the surface of the Earth, and is unique in the extent of its occurrence in all three phases: solid, liquid and gaseous. Its formative influence on the nature of the earth's surface, on the behaviour of earth materials, and its role in the complex pattern of transfers of energy and mass in the ground and atmosphere make water is a central component of study in the earth siences [108].

Pure water at atmospheric pressure freezes and at 0°C, and this temperature is usually named freezing point of water. However in soils water does not freeze at 0°C since it is not free of solutes and not subjected to the atmospheric pressure. Freeze and thaw takes place over a range of temperature. Therefore phase transition, between solid and liquid, is the basic element in understanding freezing and thawing soil materials. To describe the behaviour of frozen ground we must consider both thermodynamics and the mechanical properties of the materials.

As a matter of fact $22.79\,10^6$ km^2, 23.9% (excluding glaciers and ice sheet) of the land surface in the Northern Hemisphere is occupied by permafrost, Fig.(1). Moreover using the 0°C and 5°C isotherms of mean monthly air temperature, the long-term average maximum extent of seasonally frozen ground is about $48.12\,10^6$ km^2 or the 50.5% of the exposed lands in the Northern Hemisphere [112]. Also, resource development and population in these areas are increasing. Freezing a volume of water without constrain expands its volume by 9%. In silty and loamy soil types where a source of water is available and temperature is lower than melting temperature segregation ice lenses can form. In presence of an adequate thermodynamic gradient and hydraulic conductivity liquid water moves through the ice lenses that will grow as long as water is supplied. The growing of the ice lenses determine the heave of the ground that can expands even of 50%. It is worth to underline that frozen soil is definitely mobile, it expands and contracts as its temperature changes. Although movements associated with freeze and thaw processes are slow, they are a threat to the structural integrity of buildings, roadways and other structures built on it. Moreover permafrost influences many facets of everyday living that are often taken for granted in warmer climates. For example in areas with seasonally frozen ground, finding water in the winter is not that difficult since the ground water does not freeze. In permafrost areas, however, most of the ground water is frozen and at the same time the chemical composition of remained waters chemical composition is different since minerals get concentrated. Problems arise also in building water pipes. These have to be protected so that water inside the pipe does not freeze and to prevent the pipes from thawing the ground. Hence the pipes have to be kept up off the ground.
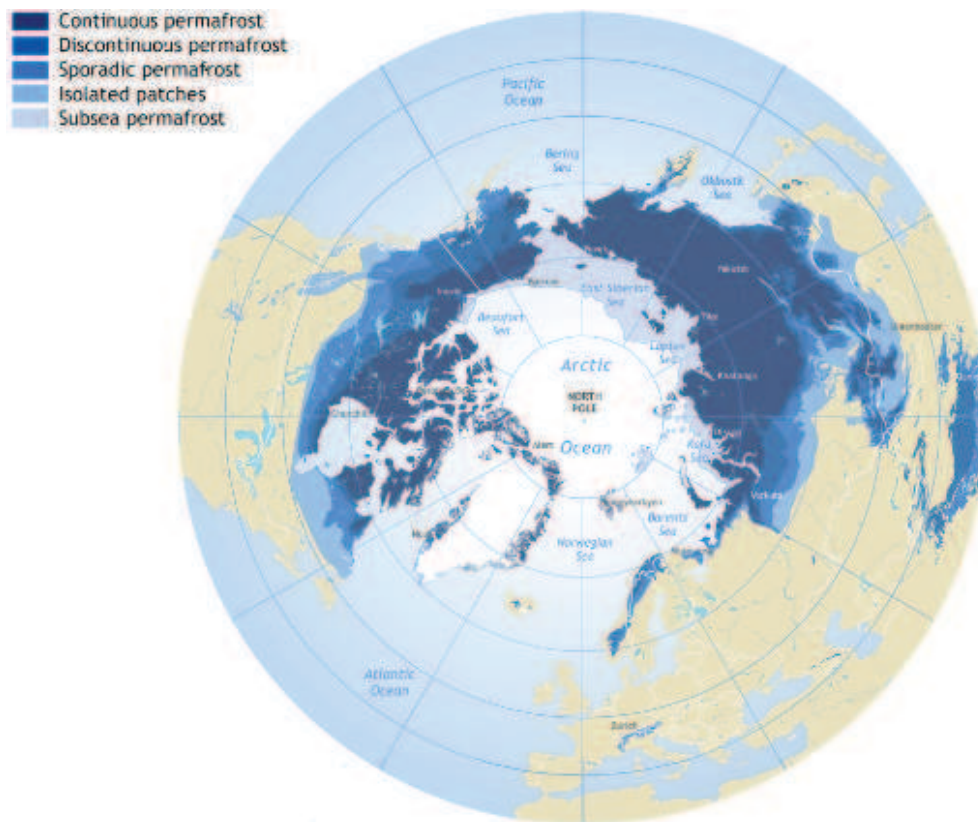
Figure 1: Permafrost occurrences in the Northern Hemisphere [7].

Initial efforts directed at building infrastructure on permafrost assumed that the frozen ground was in thermal equilibrium. It is now obvious that because of climatic change permafrost is not in thermal equilibrium. Instead, it is warming in many areas and this needs to be considered in the present design criteria. Also, the economic impact in terms of loss of serviceability and ongoing maintenance gave a further decisive boost in studying frozen ground. Beyond the World Climate Research Programme (WCRP) together with the Climate and cryospheric (CliC) Project recently recognized that better understanding of the interactions and feedback of the land/cryosphere system and their parametrization within climate and hydrological models are needed [3]. Moreover freezing and thawing processes have a considerable impact an ecosystem diversity and productivity. It was pointed out that greenhouse gas exchange between the atmosphere and the land surface may be minimal when the soil is frozen but is accentuated in the early spring following thaw [112], hence there is a direct feedback with the climate system.

Just as it took a long time for permafrost to develop, it will take a long time for it to completely thaw; but during the long and persistent process of thawing, climate consequences can impact our daily lives.

2.2 WHAT PERMAFROST MEANS

The first term used to describe permanently frozen ground was "permanent frost"; actually, in an ordinary man's view, it properly described the phenomenon which did not change during the lives of generations of people connected with the area of its occurrence. But it is obvious that the term could not be accepted from a scientific point of view. Thus it was replaced by the term "perennial-frozen-permafrost" which much better reflects a relation between continuously frozen ground and time [19]. Now permafrost means ground (soil or rock and included ice and organic material) that remains at or below 0°C for at least two consecutive years [101]. Permafrost is only defined on a temperature criterion, as a thermal state of the lithosphere and of anything inside it. So it is worth to point out three significant consequences for proper understanding of what permafrost is.

First, not all frozen ground is permafrost. Freezing conditions in the surface layers of the earth occur not only in the polar regions, but also in temperate zones, and at high elevation even in the tropics. Moreover the existence of frozen layers varies from a few hours in low latitudes to thousands of years in high latitudes. So to distinguish the ground that thaws annually from permafrost we call the first one seasonal frost. This distinctions could be misleading. As a matter of fact also the layer above permafrost is characterized by freeze-thaw cycles that follows the seasonal pattern. Below this seasonal 'active' surface there is permafrost.

Second, consistent with the definition permafrost may not necessarily contains water. We can distinguish between permafrost in which there is liquid water and dry permafrost.Dry permafrost refers to permafrost contains neither free water nor ice [101]. This definition is not absolutely accurate as ice itself is also dry and a negligible quantity of moisture in the form of interfacial water may be present. It is important to underline that, in agreement with the IPA's definition, dry permafrost is stable since it can not change.

Third, if there is water in the permafrost body, it can be frozen, unfrozen or only partially frozen. It is worth making clear the difference between the temperature (i.e. thermal) and state (i.e. frozen or unfrozen) conditions of permafrost. Actually not all water freezes at 0°C. Ground water contains some dissolved salts, which lower its free energy. Because of this solution has a lower free energy than pure water, for ice to form it must have a different free energy from ice forming in pure water. Hence only at some temperature below 0°C the free energy of ice is lower than that of the solution, such that ice forms from the solution. This is called depression of the free energy point. However, since the concentration of dissolved salts in the soil water is so weak, the melting point is usually 0.1°C below 0°C. Both capillarity and adsorption play a more relevant role to lower the melting point of soil water. Capillarity is an effect associated with molecular forces at the interface between phases, when the interface is confined. The rise of water in capillary tubes follows from the confinement of the interface (the meniscus) between the air and water. The rise is greater as the tube diameter is smaller. This suction can be equated with a decrease in free energy relative to normal, or "free" water at the same temperature. The regions between soil grains can be viewed as capillary tubes and so the free energy falls. Adsorption reduces

the free energy too, but it is due to the influence of forces emanating from the mineral particle surfaces. Of course this effect affects only a thin layer of water on the particles, the so called adsorbed layer.

As a consequence of these effects water in soils does not freeze at 0°C but over a range of temperature that fulfills the thermodynamic equilibrium. The melting temperature changes it is always below 0°C. This means that at any particular temperature there is a particular quantity of water that does not freeze. The system is characterized by a delicate equilibrium state among soil temperature, ice and water content and just a small variation in energy and mass balance will force the system to reach another equilibrium state. Therefore, it is essential to describe clearly the actual state of the water in a particular soil within the current temperature regime [5].

2.3 CLIMATE AND FROZEN GROUND

According to the definition of permafrost, the element of permanency in permafrost is bonded to the equilibrium between low ground temperatures and climatic and other conditions. For that reason studying permafrost requires to understand the ground temperature regime.

In the upper layer of the earth the thermal regime is controlled by exchanges of heat and moisture between the atmosphere and the ground surface, together with the influence of ground thermal properties. The fluctuations of the surface temperature are the consequence of climatic and weather changes. The thermal properties of the ground control the downward propagation of these fluctuations. The study of the thermal regime of the ground can not be restricted to the analysis of these energy fluxes. Actually local surface conditions such as snow cover, the vegetation canopy, topography, play a significant role to determine the surface temperature.

Lockwood (1979) [60] provides the follow useful scheme to visualize the interactions occurring in the surface boundary layer that affect ground temperature.

2.3.1 The surface energy balance

The starting point to quantify the variations in ground thermal conditions is the surface energy balance. This is determined by the net radiation (Q_*), which is the balance of the short and long wave radiation income and outcome. This difference between incoming and outgoing radiative energy gives rise to other forms of heat transfer at the earth's surface. The processes of evaporation or condensation involve the absorption or release of latent heat by water, and the energy used in these processes in represented by (Q_{LE}). (Q_H) the transfer of sensible heat due to the temperature gradient between the atmosphere and the ground surface, convective flux, and that due to wind, advective flux. At last the conduction of heat into the ground (Q_G). This includes the heat flux due to the local thermal gradient in the ground and the heat flux associated with the water flow.
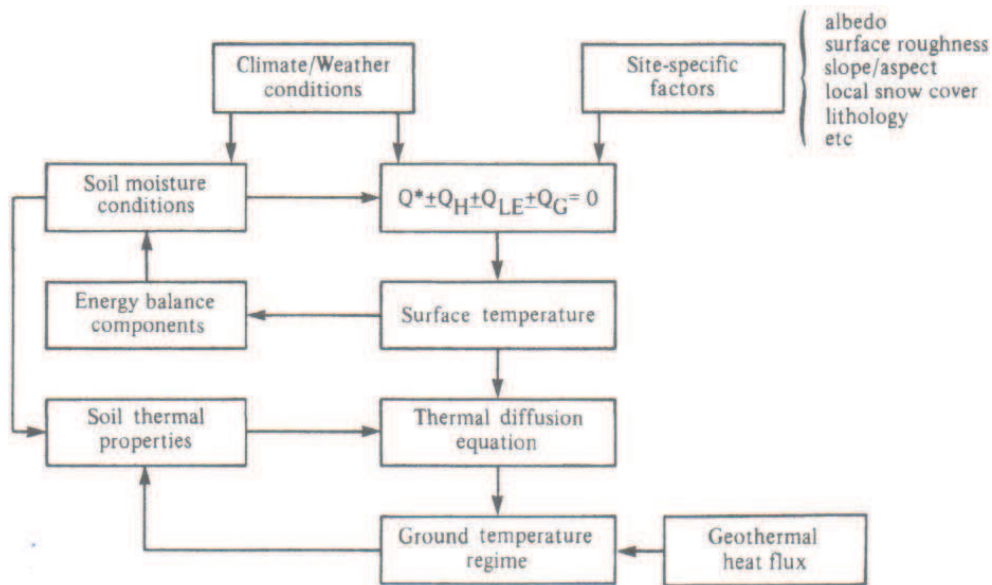
Figure 2: Flow diagram of climate-ground thermal interaction (Lockwood, 1979).

According to the conservation principle, energy must be conserved. The balance of these energy fluxes determines the surface temperature of the ground.

It is evident that all these processes are characterized by their own temporally variability scales. So we may speak of an hourly, daily, monthly, yearly energy budget.

In middle latitudes, high elevation regions such as the Alps, the Rockies, and the mountain of Scandinavia the winters are not particularly cold nor the summers warm so there is marked diurnal cycles. This means that when the ground temperatures are around 0°C the most superficial layer of the ground freeze and thaw.

However, because permafrost definition requires the ground to be frozen for more than one year so what is important for permafrost is the annual thermal regime. This is due to the changing pattern of the season. In summer months the ground accumulates heat that will be more or less completely lost during the winter season. Hence over a year the sum of ingoing and outgoing heat fluxes commonly approach to zero. The annual regime is dominant in areas characterized by a well sharp seasonal pattern such as high latitude. It is significant to differentiate between continental and maritime climates. These two kinds of climates are due to the contrast in the thermal response of land and water body surfaces. Continental climates exhibits a large annual range in air temperatures. Land surfaces heat and cool rapidly since soil and rock have low specific heats. Moreover continental climate regions present low rainfall and snowfall that enhance the rapid heating of the ground surface. So in markedly continental climates, winters may be very cold, but the counteracting of warm summers, means that annual frost penetration will be deep only when the mean temperature is within a few degrees of 0°C [108]. On the contrary in a maritime climate region the closeness of a significant water body determines a smaller annual range in air temperature and a high rainfall regime that affects the exchange of latent

heat between the ground surface and the atmosphere. Hence there will be no significant freezing of the ground unless the mean ground temperature is less than about 5°C [108].

It should be pointed out that the element of permanency in permafrost is bonded to the equilibrium temperature below 0°C, while the energy balance over years determines the aggradation or degradation of permafrost. Both of them has the effect of changing the thickness of permafrost and its equilibrium temperature. When the heat balance is negative, aggradation of permafrost, there is an increase in its thickness and the temperature falls further. On the contrary the positive heat budget leads to a decrease of permafrost thickness and temperature raising.

The term microclimate refers to the interaction of site-specific factors with climate. It is the microclimate which is ultimately of importance to ground thermal conditions, since a difference in the surface characteristics will cause a change in the exchange of heat between the atmosphere and the ground, with significant effects for the ground surface [108]. So the mean annual ground temperature usually differ by several degrees from mean air temperatures. Moreover site-specific factors present an high spatial variability. Therefore in a same area at the same boundary condition changes of site-specific factors determine a range in ground thermal conditions that we can observe among several degree of latitude. The effects of these changes are more significant where the ground temperature is close to 0°C since they determine whether permafrost is present or not.

The primary influences of the vegetation canopy are the reduction of solar radiation reaching the ground surface and the variable effects on the depth and persistence of snow cover [63]. In addition, interception of precipitation and transpiration by the canopy influence the ground thermal regime through the water balance [84]. Rouse (1984) [89] highlighted the large aerodynamic roughness of the forest producing greater turbulent exchange with the atmosphere.

Seasonal snow cover is one of the primary factors influencing the ground thermal regime in cold regions. This is because snow is an insulator compared to other natural materials. Therefore in winter months snow cover reduces the heat loss leading to raise of mean annual ground temperatures. Gold (1963) [27] concluded that snow cover was the principal reason that mean annual ground temperature can be many degrees warmer than the mean annual air temperature in cold regions. Where air temperature is close to 0°C, seasonal snow cover can be responsible for the absence of permafrost in certain locations [113]. The influence of the seasonal snow cover on the surface thermal regime can be explained by the following factors. Firstly, the snow cover presents a high surface albedo. It is defined as the ratio of all-wavelength solar radiation reflected by the surface to that that incident upon it [6]. As consequence the absorbed solar energy is reduced and hence the snow surface too. The effect of albedo is much more evident when the global radiation is greater. Since albedo depends on snow cover characteristics it is strongly affected by the metamorphism of snow. It is higher for fresh snow and then it decreases with snow melting. Secondly, over the thermal infrared part of the spectrum, snow acts almost as a "black-

body" [114]. This is due to the high value of emissivity. For a cold dry and clear-sky condition, higher emissivity of snow surface may result in surface cooling and very often the development of a low-level temperature inversion [92]. On the other hand, higher emissivity on the snow surface also implies higher absorptivity of snow surface as defined by Kirchoff's law [104]. For a relativity wet atmosphere with cloud sky, atmospheric downwelling long-wawe radiation is strong and the snow may adsorb more energy because of its higher absorptivity, resulting in higher surface temperature. The over-all effect of snow emissivity and absorptivity on snow surface temperature largely depends on overlying atmospheric conditions [114]. Thirdly, a large fraction of the snow layer is filled with air and so the thermal conductivity is extremely low [114]. Like the albedo the thermal conductivity changes with snow metamorphism. During snow metamorphism the density increases and as a consequence the thermal conductivity too. At last the net effect of the seasonal snow cover on the ground thermal regime and its magnitude depends upon the timing, duration, accumulation, melting processes of the seasonal snow cover, and its physical characteristics [114].

The presence of organic material leads to lower mean annual temperature. This is effect is due to the marked seasonal variation in the thermal properties of peat. In summer peat is usually dry, because of evaporation, and its thermal conductivity is very low. Therefore warming of the ground is inhibited. On the contrary, in fall peat becomes quite moist and its thermal conductivity raises up. Moreover when it freezes the conductivity becomes higher and the ground can cool rapidly. Peat presents a behaviour that is the opposite of the snow. As a consequence permafrost may occur in locations where the mean annual surface temperature is actually above 0°C [58][121].

It is worth to highlight that changes in the surface conditions can modify the thermal regime of the ground. This is of great importance in connection with human activities. Usually surface changes will lead to an increase in the mean summer surface temperature [74], eventually accompanied by melting in the upper layer of permafrost. This leads to a change in the mechanical properties of the soil. Moreover when soils thaw melt water is produced at a rate controlled by thermal processes, whereas the dissipation of water depends on the discharge capacity of the soil [76]. However there are occasion where the surface changes bring about ground cooling. This may happen as a consequence of lake drainage or river shifting [94]. The clearance of snow due to the presence of highways or airfield may serve to stabilize the thermal condition of the permafrost but may also lead to icing problems on highways [108].

As pointed out by Lockwood in his diagram Fig.(2) soil moisture is a significant factor in the ground temperature regime. It affects both the surface energy balance and the ground thermal properties.

A wet surface is one from which evaporation can take place, and it is the most common type of surface found in nature. The evaporation is the change of water or ice to vapour, an it proceeds continuously from water, soil, snow and ice. The rate of evaporation depends on prevailing weather and climatic conditions and on the availability of water at the surface. The transpiration one is related to the soil water extracted by plant roots, and discharged as

vapour into the air as a product of photosynthesis. Even though this two processes are different usually they are referred as evapotranspiration. The importance of evapotranspiration on the surface energy balance is due to water thermal properties. The high specific heat capacity allows water to absorb and release a very high quantity of heat with slightly variation in its temperature. Moreover evaporation of water will subtract a huge quantity of heat from the ground because of the high heat of vaporization.

2.3.2 Ground thermal regime

The systematic seasonal fluctuation of the heat fluxes between the ground surface and the atmosphere imparts a temperature wave to the ground surface that propagates downward to the Earth. The temperature at depth oscillates with the same (annual) frequency as the surface temperature, but with an amplitude that diminishes and a phase lag that increases with depth [108]. At a certain depth the temperature remains almost constant. This is the so-called'zero annual amplitude' and depends on the the nature of soil materials, varying directly with bulk density and moisture content through thermal conductivity. Soil temperature varies diurnally and annually following changes in surface ground temperature. The surface regime, is the major factor affecting the ground thermal regime. However, ground thermal properties, and at great depths, the heat flowing from the earth's interior serves to modify the effects of surface temperature [108]. The soil heat flux relates to the nature of soil materials, varying directly with bulk density and moisture content through thermal conductivity.

Ground temperatures are, for the most part, determined by conductive heat transfer. The heat flux downward or upward is controlled by the gradient of temperature in soils. Dealing with the heat flux in the ground requires to know the soil thermal properties. The ground is not an homogeneous solid, but presents different layers whose thermal properties vary with its composition. Besides this heterogeneity, the composition of naturally occurring soil varies continuously, chiefly because of changes in the amount and phase of water at various locations [21]. The amount and phase of ground water is attributed to two physical mechanisms. The first mechanism is represented by the soil freezing characteristic curve, which establishes a relationship between the temperature and unfrozen water content in frozen soil. The second one is the Clapeyron equation, which predicts that the melting point of water will decrease to somewhat below the melting point of bulk water because of the presence of suction. The presence of ice and water close to their transition temperature has a dominant effect on the thermal properties of frozen soils. As a matter of fact small changes in the ground temperature lead to significant variations in the thermal properties of the soil. When water changes to ice, its conductivity increases four-fold, its mass heat capacity decrease by half, and it releases heat equivalent to that required to raise the temperature of an equal volume of rock by about 150°C [26]. Latent heat keep soil near 0°C for a considerable length of time in a refreezing or thawing active layer [78]. Thus, the latent heat of fusion released or adsorbed during pore phase change increases the thermal inertia

of the subsurface, and at temperatures close to the freezing point, this latent heat can dominate conductive heat transport [45].

Hinkel and Outcalt (1993) [36] have presented spectral data that indicate soil temperature vary diurnal, annual and other frequencies. While the diurnal and annual cycles are associated with heat conduction following well recognized variations in surface temperature, the various other frequencies have been attributed to non-conductive processes. In particular, infiltration may lead to heat transfer following snowmelt or summer storms [35]. Wave periods of less than a day have been attributed to redistribution of heat within the soil by evaporation, movement of vapour, and condensation, collectively termed "distillation" [37].

Another mechanism that influences the ground thermal regime is due to the groundwater flow. Thanks to the freezing point depression groundwater may remains unfrozen at temperature below 0°C. Thus, especially in warm permafrost there is pore water that provides suitable media for active groundwater system [53]. However, the groundwater flow in permafrost regions is strongly affected by the ground temperature since the presence of pore ice reduces the hydraulic conductivity of the soil [23]. Convection may be an important mechanism of heat transfer in organic soils, sands or gravels since they present per se a high hydraulic conductivity. On the contrary convection may be much less significant in finely grained materials that present a lower hydraulic conductivity[86]. The interest in studying groundwater in permafrost has been recently renewed due to the potential interactions between climate change, permafrost degradation, and groundwater flow [65]. The rise of temperature may cause that the seasonal frost does not reach the top of permafrost. The unfrozen layer between the active layer and permafrost is named talik [23]. Talik has significant influence, as a heat source, on the thermal regime of neighbouring seasonal frost or permafrost in winter [59]. This is due to the temperature of the talik that is always above the freezing point and hence these zones can provide conduits for water which is associated a huge amount of heat flux thanks to its high heat capacity and latent heat of fusion. At the beginning, the presence of ice-free regions in otherwise continuous permafrost allow ground water to flow laterally above the permafrost and then to flow downward below recharge areas as taliks deepen. Once the taliks fully penetrate the permafrost allow groundwater to pass vertically through the permafrost layer. These preferentials pathways enhance the heat advection that becomes greater than the heat conduction alone. As a consequence, gothermally warmed water from below or relative warm groundwater recharge from above promote the growth of talik network by accelerating thawing along the periphery of residual permafrost. It is clear as the degradation of permafrost is a selfuelling process. The surface recharge depends on the presence of a surface water body, the topography that determine the run-off, and snow cover where it is present. Snow cover prevents the ground to cool down and when it melts, provides a source of water that can infiltrate in the ground. Moving downward in the ground, water loses heat due to conduction and as it thaws ground ice. Thus, the ability of recharge water to thaw permafrost is greatly reduced, making sub- permafrost flow less effective in regional permafrost thaw. About geothermally

warmed groundwater its contribute to thaw permafrost is less relevant than surface recharge since it is strongly affected by natural convection, on regional topographic hydraulic gradients and on hydrogeologic structure. It is worth to underline that there are two types of groundwater flow that enhance thaw rates: flow around the periphery of permafrost bodies, and flow through permafrost bodies. The first one is much more important in determining the spatial pattern of talik network, whilst the second one in enhancing the early stage thaw. The influence of heat advection flux is much more significant in warm permafrost (temperature is close to 0°C) thanks to the ease with which talik networks may form. In cold permafrost the groundwater flow is lower and thawing is mainly controlled by heat conduction.
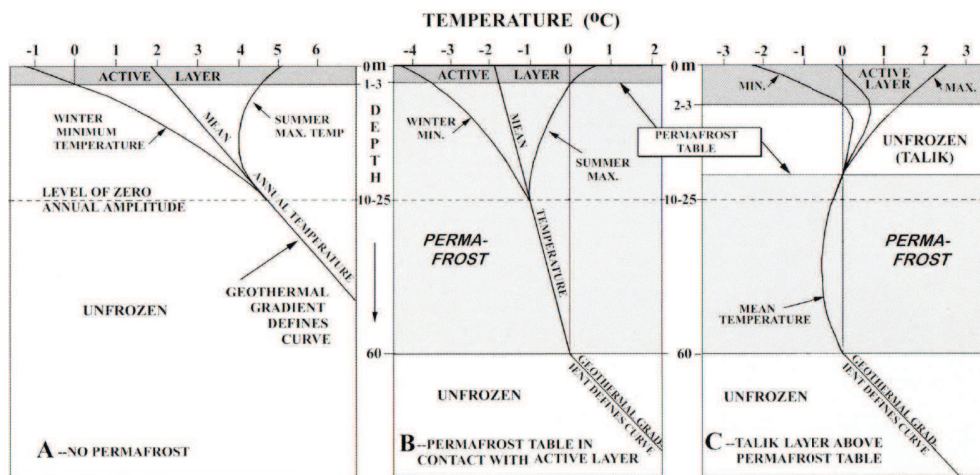

Figure 3: Schematic plots of ground temperature where: A–no permafrost is present the active layer, B–the permafrost table is in contact with the bottom of the active layer, and C–the nonequilibrium situation where climatic change or other cause has melted the upper portion of the permafrost to leave an unfrozen layer (talik) between of the active layer and the permafrost table [18].

2.4 PERMAFROST PROBLEMS

The major awareness of problems related to the changes of geocryological conditions are closely related to the intense pace of economic development of the territories within the permafrost region [110]. Engineering geocryology as a branch of geocryology studies the freezing ground of the Earth's crust as an environment for human life and activity [110]. Among the main problems of engineering geocryology is the engineering-geological background for design, construction and operation of different engineering structures and undertakings within the permafrost region. The aim is to provide and select the most reliable and economic means of development of an area.

Usually geologist classify the materials of the earth according to their lithological nature ignoring the presence of water. Water is fluid and its amount is continuously changing. However when frozen is not so nearly ephemeral ice and/or water content get greater prominence than the description of the

other mineral of the ground. This is because the ice is not stable since it is close to its melting point, while all other materials are hundreds of degrees below theirs [108]. Therefore it is worth to know where the ground, the soils and rocks, are actually frozen. Changes in the energy balance of the ground determine consequences on geocryological condition such as increase or decrease of mean annual ground temperature, and of seasonal or perennial ground thawing or freezing. These consequences are much more significant as more frozen ground contains large quantities of moisture. It is worth to point out that seasonally frozen ground causes many problems as permafrost does. For what concerns permafrost we must also distinguish between warm and cold permafrost since their response to changes in the energy balance is different. In presence of warm permafrost there is not a lot of room for the ground to warm up before impacts on permafrost takes place, on the contrary cold permafrost has some room to accept some climate change before its metamorphism.

Energy balance changes, and hence geocryological conditions changes, may be due to both climate warming and technological impact due to human activities.

As recognized by the IPPC, global climate warming is an ongoing phenomenon, and estimates for the next century merely reflect its continuation. The increase of mean air temperature and precipitation leads permafrost degradation taking place over large areas with significant biogeochemical impacts on hydrology, ecology, and green house gases. There is a considerable concern that permafrost thaw could act as a positive feedback mechanism to future climate change by releasing carbon and methane stored in northern soils [32]. Currently, Artic and boreal soils contain about 40% of the global terrestrial carbon, and this undergoes very little decomposition [28]. Thus, in the recent past, soil in northern muskeg and peatlands has provided storage for global carbon [64]. However, climate change can accelerate the rate of decomposition in these organic soils and transform northern soils from a global carbon sink to a global carbon source [87]. Moreover permafrost degradation enhances hydraulic exchanges between surface water bodies and suprapermafrost groundwater. Thus aquifer activation arising from permafrost degradation may increase baseflow to rivers and lakes and reduce seasonal variability in river flows [67]. The quality of groundwater will likely also be affected by degrading permafrost, because the presence of permafrost affects the residence time in aquifers and thus the time available for biogeochemical reactions between the pore water and soil particles [107] Weakened soil properties due to permafrost degradation can also alter ecosystems. For example, previously forested regions are being converted to bogs and fens due to a removal of their soil foundation and other altered physical and thermal conditions [42].

Of course these changes due climate warming may have direcet impacts on life of those communities that lives in cold regions. However against this climate variability nobody wants to make additional investment without being certain of its effectiveness tomorrow. Therefore, consideration of global warming in engineering practices will become realistic only after each scenario is characterized by the probability of its realization and hence the hazard is known [49].

For what concern the human activities, their effects on geocryological condition depends on the duration and the size of the area where they occur. According to the duration they can be continuous, as determined by the length of time the newly created technological landscape has existed in the length of time the newly created technological landscape has existed in the designated state and regime; temporal when take place for a number of years. Temporal and especially continuous impacts can cause a change of ground heat state at greater depths even leading to the complete thawing of the permafrost [110]. On the other hand, impacts that lasts not more than one season such as release of water on the surface, modification in thickness and density of the snow cover may affect the seasonal thawing depth. Further more it has been suggested reversible, irreversible and destructive disturbances be distinguished according to the character of the response of the geological environment.

One of the main features of design, construction and operation of engineering structures within the permafrost regions is the necessity to take into account and to regulate heat exchange between the ground, the construction and the environment. Change of ground thermal and moisture conditions in the course of economic development especially in connection with the temperature going through $0°C$, causes changes of ground composition, of structural properties as well as of strength, bearing capacity and compressibility, of heaving and shrinkage stress and deformations in freezing and thawing ground, of workability within the permafrost zone as far as excavation work and mining are concerned, of intensity of thermal erosion, icing, thermokarst, solifluction and other cryogenic processes and phenomena which can turn some terrains into badlands.

Thus there exist specific conditions for construction or for any other economic activity within the permafrost regions. Attempts to apply the standard methods and techniques for construction usable outside the permafrost zone to the regions where frozen ground is widespread often lead to inadequate and sometimes even to catastrophic consequences. For this purpose in 1998 the Canadian Panel on Energy Research and Development published guidelines for permafrost design affected by climate change [1]. The report describes a screening process to account for these uncertainties. The aim is to determine the vulnerability of the project toward climate changes. It concludes that the effort required accounting for climate change effects will not exceed what would normally be undertaken, and may possible be incorporated into an existing design process with little modification [34]. In contrast to other regions, the design life of a structure built in a permafrost environment should be planned to be 30 to 50 years, rather than 100 years [34]. In addiction, monitoring and adaptation strategies have to be implemented, that will later permit modifications to be made to the structure, as required. Since future climatic trends are difficult to predict, sensitive structures have to be re-assessed on regular basis, as new trends and better models become available [34].

In contrast to artic regions, where infrastructure in permafrost includes entire communities [38], there are no large permanently inhabited settlement construct on European mountain permafrost [34]. However, densely populated settlements and transportation routes at lower altitudes may be
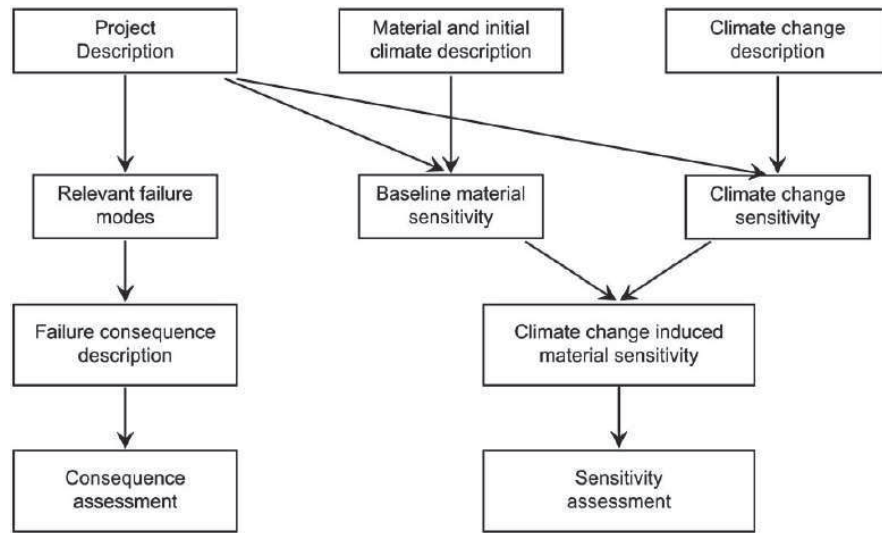
Figure 4: Schematic of climate change screening process [1].

severely affected by processes occurring in permafrost terrain, requiring engineering solutions such as retention dams [47] and the establishment of hazard maps for improved land-use management [96]. Much of the infrastructure located directly on or in mountain permafrost pertains either to tourism, communication or power-related industries and is of high economic and social significance [34]. A greater frequency of extreme summers, such as that experienced in Europe in 2003, is likely to lead to significant increases in seasonal thaw depth and problems related to permafrost may become an increasing cost factor in the maintenance or construction of high-mountain infrastructure [43]. The presence of permafrost in high alpine environments increases the difficulty in dealing with the analysis of local ground movements. In fact, the current approach on analyzing slope deformations and landslides has often been hydro-mechanical, i.e. the tensions and deformations have normally been related to water pressure and mechanical stress-strain relationship[91]. In presence of permafrost it is necessary to enhance this approach taking into account the thermal regime of the ground [34]. The thermal regime in mountain regions is strongly affected by the orography and the high variability due to local factors. Moreover the the human activities such as tunnels [106], avalanches defence structures [98], and technical snow modern ski piste preparation [22] alter the ground temperature. Rock glaciers are able to displace debris volumes of the order of 10^3 to 10^4 m^3 per millennium, and the current trend towards higher ground temperatures may be responsible for an apparent increase in creep rates in many Alpine rock glaciers [34]. Structures, such as cableways constructed where permafrost creep is active, clearly run the risk of increased maintenance costs and in the absence of appropriate engineering solutions may eventually become unserviceable [34]. Another problem is related to warming permafrost in rock walls. In this case atmospheric and ground temperatures are strongly coupled on steep mountain bedrock slopes due to the absence of an insulating interface of snow, vegetation and soil material [34]. Hence climatically-driven permafrost degradation can lead to increased instability leading to a serious increase in hazard and risk.

3

PHYSICS AND EQUATIONS OF WATER IN SOILS ACCORDING TO MUALEM'S CONCEPTUALIZATION

3.1 YOUNG–LAPLACE EQUATION

The derivation of the Young-Laplace equation will be performed following Dall'Amico's work [17].

The capillary tube is characterized by the presence of curved interfaces between the phases and thus the thermodynamical equilibrium depends by the curvature of the interface, i.e. the surface tension existing between the two phases. Let us imagine a single capillary where liquid water is in equilibrium with its vapor and air. By a simple equilibrium of forces, one obtains:

$$p_a \pi r^2 = p_w \pi r^2 + 2\pi r \gamma_{aw} \cos \alpha \tag{1}$$

where p_a, p_w are the pressure of the gaseous portion and of water respectively, α is the contact angle and γ_{aw} is the surface tension between air and water. Dividing all by πr^2

$$p_a = p_w + 2\gamma_{aw} \frac{\cos \alpha}{r} \tag{2}$$

and the water pressure p_w becomes:

$$p_w = p_a - 2\gamma_{aw} \frac{\cos \alpha}{r} \tag{3}$$

Equation 3, usually known as Young-Laplace's equation completely describes the equilibrium state including the interface shape, and the contact angle in capillaries.

The same equation may be derived by the more general formulation, if the surface area of the interface separating water and air is assumed to be just a function of the water volume, $A_{aw}() := A_{wa}(V_w)$, where A_{wa} is the area of the separation surface between water and air, and V_w is the volume of the water droplet. Then

$$p_w = p_a - \gamma_{aw} \frac{\partial A_{aw}()}{\partial V_w} \tag{4}$$

In a saturated soil all the pores are filled with water and no air-water separation surface is present. In this case the water pressure totals $p_w = p_a + \rho_w gh$, where h is the water column height above the point, and depends just on the gravitational gradient. In an unsaturated soil, on the other hand, the presence of the menisci creates a negative pressure according to Eq.(3). This pressure divided by $\rho_w g$, represents the energy, up to the Darcy scale, belonging to the water in the capillaries. Integrating this energy in a representative elementary volume and dividing by the total volume, one

obtains the mean energy of the water in the volume, considering all the radius in the various capillaries. This value is called soil suction and is usually referred to as ψ. By extending the Young-Laplace equation to the soil pores, it is clear that with increasing negative pressures, increasingly smaller pores are being emptied.

3.2 WATER IN SOILS

3.2.1 Porosity and pore–size distribution

Almost everything that occurs in the soil such as the movement of fluids, air, the transport and the reaction of chemicals is strongly affected by voids space, that portion of the soil's volume that is not occupied by or isolated by solid material [75]. Because soil does not contain discrete objects with obvious boundaries that could be called individual pores, the precise delineation of a pore unavoidably requires artificial, subjectively established distinctions [75]. To overcome this problem, it is widely accepted to consider the pore space as a collection of channels through which fluid can flow [75]. The pore space can be characterized by porosity ϕ and the pore-size distribution $f(r)$, in which r is a representative radius of pores [75].

Porosity ϕ is defined as the fraction of the total soil volume that is taken up by the pore space. It is a single-value that ranges between 0 and 1. Porosity depends on several factor such as packing density, the shape of particles, cementing, and the presence of organic matters. Usually porosity is conceptually partitioned in two components, most commonly called textural and structural porosity. The first one is the value the porosity would have if the arrangement of the particles were random. On the other hand the structural components represent the porosity due to non random structural influences, including macropores. Porosity defines the upper limit of the volumetric water content θ. Pore-size distribution is the relative abundance of each pore size in a representative volume of soil. It can be represented with a function $f(r)$, which has a value proportional to the combined volume of all pores whose radius is within an infinitesimal range centered on r [75].

Actually soils exhibit a variety of heterogeneities, such as fractures, fissures, cracks, and macropores or interaggregate pores [25]. Since the porosity provides a measure of the total volume of voids, one can not be aware of the soil's structure just looking at it. On the contrary, the knowledge of the pore-size distribution may give a much greater understanding of the soil's structure. This has a significant importance in order to understand all those processes occur with in the soil. Additionally, the pore size distribution affects solute convection similarly to hydraulic conductivity, and solute dispersion, which is expected to be greater for a broader pore-size distribution [75].

The smaller pores are associated with longer residence times and grater relative surface area, but most solutes may go quickly through the large pores with minimal opportunity to react [75].

On the other hand, macropores represent preferentials paths for the water flow and thus for solutes (i.e. nutrients and contaminants) dissolved in it

[56]. Furthermore van der Kamp et al. [100] pointed out the importance of macropores on infiltration rate within frozen soils. This is much more significant during the snowmelt [120] when the unsaturated large macropores allow an infiltration capacities exceeding the snowmelt rates. Thus in soils which have plentiful macropores, these have a positive feedback on the groundwater recharge processes that is much greater than that occur in soil which have little or no macropores where indeed snowmelt tends to run off over the surface [39]. Furthermore, the temperature of the frozen soils is about 0°C and thus the enhanced heat advection due to macropores, strongly affect the energy balance. As a matter of fact, the water flow carrying a significant amount of heat may lead ice thawing which in turn releases the latent heat of fusion with a positive feedback on the energy balance.

Natural or artificial soil processes create and destroy pores, can induce changes in their size and other attributes. Thus porosity and pore-size distribution may vary not only in space but also in time; as well these changes have consequences on what occur within the soil.

3.2.2 The volume conservation

Let us consider a rigid control volume of soil V_c. Generally it is a composite of three different constituents, Fig.(5),: (i) soil particles, (ii) liquid water, (iii) and gas or air. The volume conservation requires:
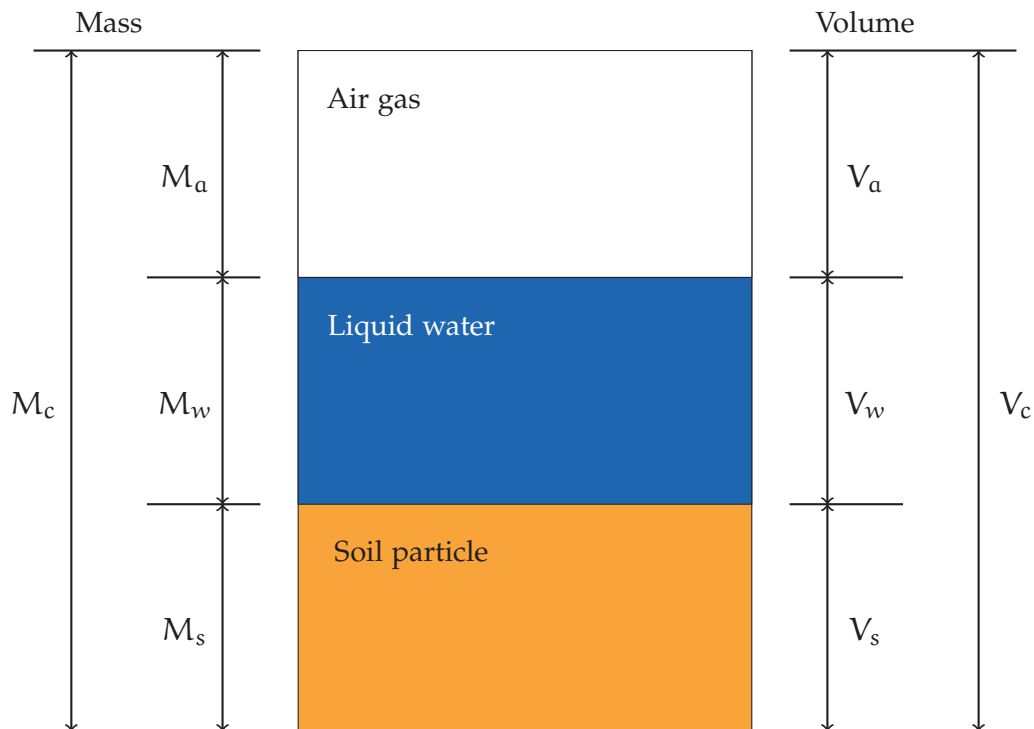

Figure 5: Unfrozen soil constituents and schematization of the control volume V_c [80].

$$V_s + V_w + V_a = V_s + V_{voids} = V_c \tag{5}$$

Let us define:

$$\phi := \frac{V_{voids}}{V_c}, \quad \theta_w := \frac{V_w}{V_c} \tag{6}$$

respectively the porosity, and the water content. Consistently with the rigid soil model, porosity is constant. In general it is assumed that the maximum dimensionless water volume θ_s that can be stored in the volume V_c is equal to the porosity ϕ. However, this is not completely true, because of entrapped air that reduces the room for stored water. Thus the saturated water content can be set $\theta_s \approx 0.85 \div 0.9\phi$.

Let us assume that $\theta_s := \phi$, then the water content has to satisfy the follow restriction:

$$0 \leqslant \theta_r \leqslant \theta \leqslant \theta_s \leqslant 1 \tag{7}$$

where θ_r is the residual water content. It is convenient to introduce the effective saturation S_e as

$$S_e = \frac{\theta - \theta_r}{\theta_s - \theta_r} \tag{8}$$

3.2.3 Unsaturated soils

When a soil is partially saturated the water present in the medium is retained on one side by the adsorbed films in contact with the solid, and on the other by capillary forces due to the curved air-liquid interface [83]. Hence it is possible to represent the soil pores by an equivalent bundle of capillaries, with identical retention properties as the real soil [51].

Since Darcy's law is independent of the size of particles or the state of packing [83], it can be extended to study the water flow in unsaturated soil. In the latter case the pressure is substituted by suction and the hydraulic conductivity depends on the water content of the soil [83]. As consequence, studying the water flow in soils and the vadose zone requires the definition of both the relationship between the water content θ and the suction ψ, and that between the unsaturated hydraulic conductivity K and ψ.

As reported by Kosugi et al. [51] basically exists two approaches to determine the soil water retention function.

The first one is based on empirical curve-fitting equations which relate the capillary soil pressure ψ to volumetric water content θ, e.g. Brook and Corey [82] and Van Genuchten [102]. A typical soil water retention curve is presented in Fig.(6). When the matric head ψ is equal to zero the water content θ is by definition equal to the saturated water content θ_s. For many soils, the value of θ will remain at θ_s for values of ψ slightly less than zero. At ψ_a the soil starts to desaturate. This is called the air-entry value, and is assumed to be inversely proportional to the maximum pore size forming a continuous network of flow paths within the soil. As ψ decreases below ψ_a, the water content usually decreases according to a S-shaped curve with an inflection point. In Fig.(6) the suction at the inflection point is denoted by ψ_i. As ψ decreases further, θ decreases seemingly asymptotically towards a soil-specific minimum water content known as the residual water content, θ_r. The concept of residual water content θ_r, is an essential but potentially problematic element in soil water retention model [51]. Historically, it was introduced assuming that the water content exhibits an asymp-
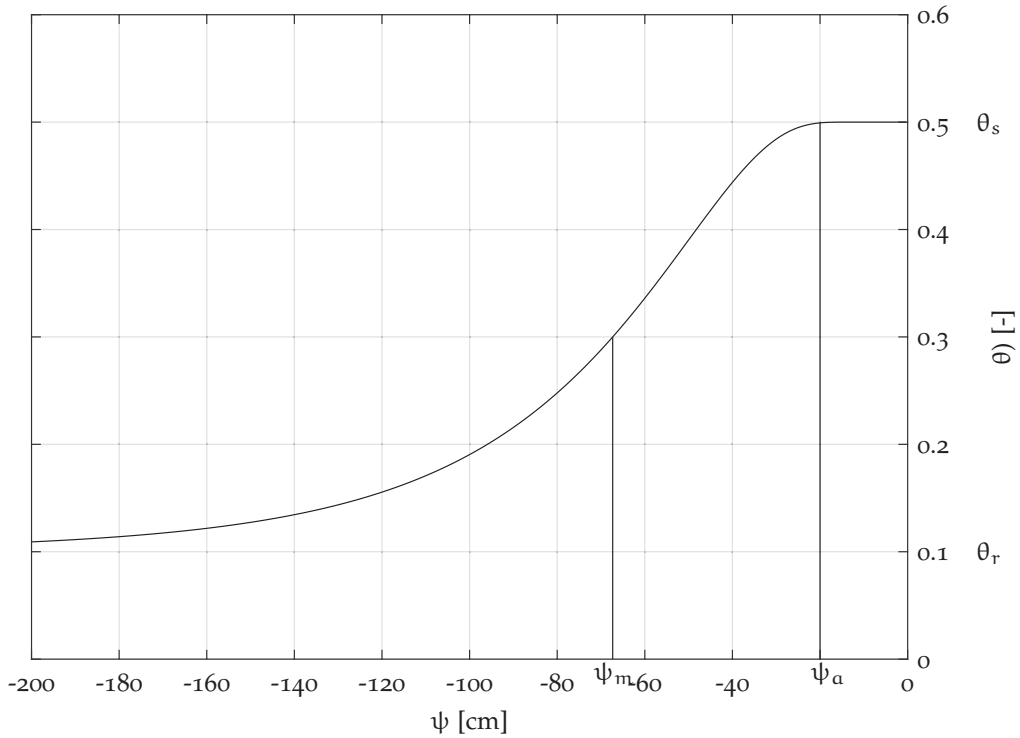
Figure 6: Schematic of a typical soil water retention curve with definitions of parameters [51].

totic behavior at low suction. This assumption causes discrepancies with measurement data in low suction range, since the water content theoretically goes to zero as the suction becomes infinitely negative [51]. Therefore, retention models that contain θ_r as a fitting parameter can be considered reliable in the range $\theta_r < \theta < \theta_s$. Besides the four parameters ψ_a, ψ_i, θ_s, and θ_r, most retention models might include parameters that have a physical basis [51]. Some these model have been developed to be compatible with models by Burdine [10] and Mualem [72] for the purpose of deriving analytical expression that can be used to predict the relative hydraulic conductivity of soil [50]. The set of the water retention model and the derived model for relative hydraulic conductivity are referred to as the combined water-retention-hydraulic-conductivity models and have been widely used for modeling purposes. Furthermore, these models are also useful for the inverse method to determine the soil hydraulic properties from transient data associated with unsaturated soil water flow, or for analyses of hysteretic phenomena that characterize both the relationship between θ-ψ and K-ψ, and spatial variability of soil hydraulic properties [50]. Despite their usefulness, these combined models do not emphasize the physical significance of their empirical parameters [50].

On the other hand, the second approach foresees to analyze the moisture characteristic on the basis of soil pore structure. As a matter of fact the particle size distributions of many soils are approximately lognormal and it seems reasonable to extends the lognormal distribution to describe the pore radius distribution [52]. As we show below the hydraulic capacity function, defined as the slope of the θ-ψ curve, is related to the pore radius distribu-

tion function by transforming variables under the assumption that there is a direct correspondence between the pore radius and the capillary pressure [52]. Therefore the hydraulic capacity is regarded as the pore capillary pressure distribution function. Unlike the previous approach based on empirical curve fitting equations, this one has the virtue that the parameters are closely related to the statistics of the pore capillary pressure distribution and that exhibits great flexibility for determining retention curves of various soils.

3.2.4 Models for soil water retention

BROOKS AND COREY [82] suggested to express the effective saturation, S_e, as a power function of ψ

$$S_e(\psi) = \begin{cases} (\psi_a/\psi)^\lambda & \psi < \psi_a \\ 1 & \psi \geqslant \psi_a \end{cases} \tag{9}$$

where ψ_a and λ are the parameters of the model that has to be properly estimated. The parameter ψ_a is the air-entry head and is assumed to be a measure of the maximum sizes of pores forming a continuos network of flow channels within a soil. The dimensionless parameter λ characterizes the pore-size distribution, and is referred to as the pore-size distribution index. Since Eq.(9) does not include an inflection point, but instead identifies a distinct air-entry value, this model usually shows excellent agreement with experimental data for soils with distinct air entry regions (J-shaped retention curves) [51].

VAN GENUCHTEN [102] suggested a S-shaped model

$$S_e(\psi) = \frac{1}{[1 + (\alpha|\psi|)^n]^m} \tag{10}$$

where α [L^{-1}] and n ($n > 1$) represent empirical parameters that are reportedly related to the inverse of bubbling pressure and the pore size distribution index ($n = \lambda + 1$), respectively, and m is related to n by $m = 1 - 1/n$. Unlike Brooks and Corey model, Van Genuchten's one does not account for the air-entry head but does have an inflection point, allowing to perform better fits for finer-textured soils and undisturbed field soils [71]. The capillary pressure at the inflection point, ψ_0, is obtained differentiating Eq.(10) twice with respect to ψ to obtain

$$\psi_0 = -\frac{m^{1-m}}{\alpha} \tag{11}$$

THREE–PARAMETER LOGNORMAL DISTRIBUTION MODEL Following Kosugi's work (1994) [52] let us define a pore-size distribution function $f(r)$, as

$$f(r) = \frac{d\theta}{dr} \tag{12}$$

where the dimension of $f(r)$ is L^{-1}, and r is the pore radius. According with Mualem's assumption [72] that the filling is ordered, before smaller pores

are filled and hence the larger ones, as well the drying, first larger pores are emptied and then the smaller one, in Eq.(12) $f(r)dr = d\theta$ represents the contribution of pores with radii $r \to r + dr$ to θ. Therefore, $f(r)dr$ is equal to the volume of pores with radii $r \to r + dr$ per unit volume of soil. The
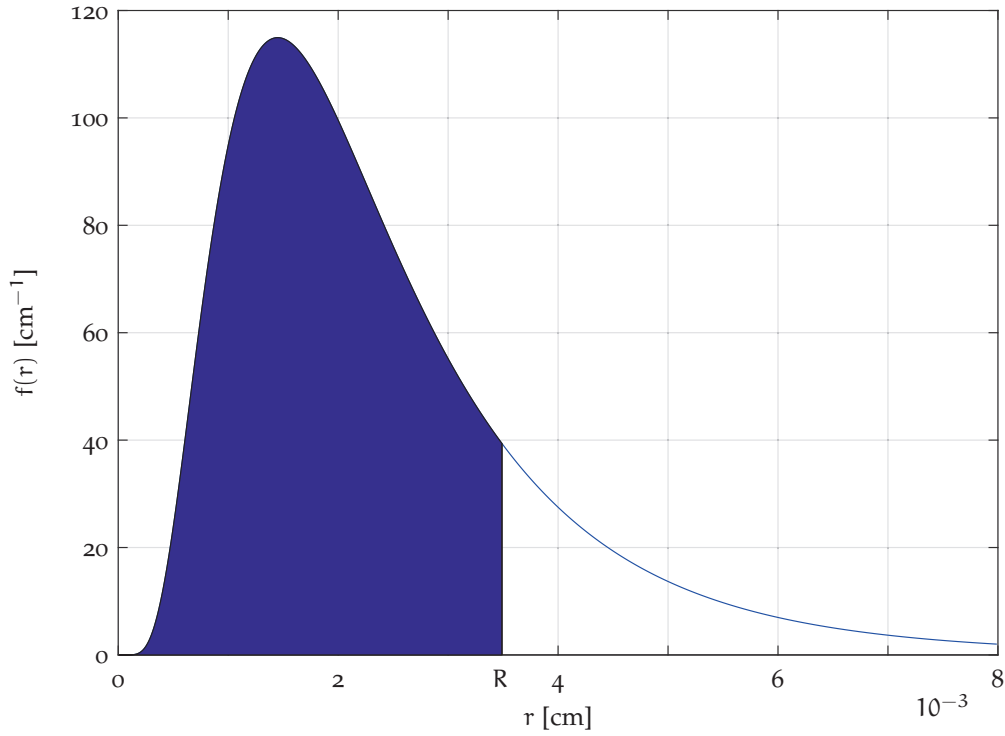

Figure 7: The pore-size distribution is described by a two-parameters lognormal distribution [50] for $\theta_s = 0.4$, $\theta_r = 0.1$, $\sigma = 0.6$, $r_m = 2.1\,10^{-3}$[cm]. According with Mualem's assumption water fulfills pores with radius $r \leqslant R$.

contribution to the volumetric water content, Fig.(7), of the water-filled pores with a radius equal to or smaller than R can be computed as

$$\theta(R) = \theta_r + \int_0^R f(r)dr \tag{13}$$

where θ_r is the residual water content. Furthermore, the relation between S_e and R is

$$S_e = \frac{1}{\theta_s - \theta_r} \int_{-0}^R f(r)dr \tag{14}$$

Assuming that the soil water is retained just by capillary forces, for each value of the radius r it is possible to determine the related matric head ψ using the Young-Laplace's equation, Eq.(3)

$$\psi(r) = -\frac{2\gamma_{aw}\cos\alpha}{\rho_w g\, r} = \frac{A}{r} \tag{15}$$

in which p_a is set to be null, and $A = -(2\gamma_{aw}\cos\alpha)/(\rho_w g)$ is a negative constant with an approximation value of $A = -1.49\,10^{-5}\,m^2$ [9]. On the basis of this direct correspondence between r and ψ, the distribution $f(r)$ is transformed into the distribution $g(\psi)$ by the following equation:

$$g(\psi) = f(r(\psi))\frac{dr}{d\psi} \tag{16}$$

Substituting Eq.(12) into Eq.(16) yields

$$g(\psi) = \frac{d\theta}{d\psi} \tag{17}$$

Hence $g(\psi)d\psi$ represents the volume of full pores in which water is retained by capillary pressure $\psi \to \psi + d\psi$ per unit volume of medium. And $g(\psi)$ can be regarded as the pore capillary pressure distribution function. From Eq.(17) it is evident that $g(\psi)$ is identical to the hydraulic capacity function:

$$c = g(\psi) = \frac{d\theta}{d\psi} = (\theta_s - \theta_r)\frac{dS_e}{d\psi} \tag{18}$$

The relationship between θ and ψ can be obtained by integrating Eq.(17) with the knowledge that $\theta = \theta_r$ when ψ goes to $-\infty$:

$$\theta(\Psi) = \theta_r + \int_{-\infty}^{\Psi} g(\psi)d\psi \tag{19}$$

where Ψ is related to R by the Young-Laplace equation. Furthermore, the relation between S_e and Ψ is

$$S_e = \frac{1}{\theta_s - \theta_r}\int_{-\infty}^{\Psi} g(\psi)d\psi \tag{20}$$

It should be noted here that $g(\psi)$ is not a probability density function but a function whose definite integral from $-\infty$ to 0 equals $\theta_s - \theta_r$. The same is true of $f(r)$.

Under unsaturated condition Eq.(14) and Eq.(20) are equivalent because of the assumption that there is a direct correspondence between the pore radius and the capillary pressure. This is not anymore true when the soil is saturated since the water pressure is no longer a function of the pore radius but it just depends on the water table level. Therefore Eq.(20) has the benefit of being used both under unsaturated condition and saturated one, whilst Eq.(14) works only under unsaturated condition. The extension of Eq.(20) to saturated condition requires some additional consideration. So far we have assumed that the soil is rigid, actually its porosity is constant as well its structure can not deform. If the soil is unsaturated this assumption is not too much limiting, but this is not anymore true under saturated condition. In the latter case the assumption of rigid soil implies that water content could not increase, and any pressure applied to the saturated soil would transmit instantaneously through the water volume. Instead, because the medium is not rigid, any pressure is transmitted with a certain speed, and pressure waves can be measured. This can be interpreted as porosity increases and at the same time pressure varies. Thus a properly extension of Richards' equation to saturated condition may be obtained extending the soil water retention curve in the field of positive pressure thank adding a term which is usually referred to as the specific specific storage. This term allows to consider the soil as an elastic medium, and hence to describe how the water content varies as pressure varies.

Kosugi proposed for $f(r)$ the following model

$$f(r) = \frac{(\theta_s - \theta_r)r_{max}}{\sqrt{2\pi}\,\sigma r(r_{max} - r)} \exp\left\{-\frac{\left[\ln\left(\frac{r}{r_{max} - r}\right) - \mu\right]^2}{2\sigma^2}\right\} \quad 0 < r < r_{max}$$

(21)

where r_{max} represents the maximum pore radius in the medium and σ and μ are dimensionless parameters ($\sigma > 0$ and $\mu > 0$). This model, Eq.(21), is derived by applying the normal distribution to the distribution of

$$\ln\left(\frac{r}{r_{max} - r}\right),$$

(22)

which is given by a transformation of $f(r)$. Here μ and σ^2 are the first moment about the origin (i.e., the mean) and the second moment about the mean (i.e., the variance, with σ as the standard deviation) of the distribution of Eq.(22), respectively. This model for the pore-size distribution has a three-parameter lognormal distribution form.

By substituting Eq.(15) and Eq.(21) into Eq.(16) and differentiating, the pore capillary pressure distribution function $g(\psi)$ can be obtained:

$$g(\psi) = \begin{cases} \dfrac{(\theta_s - \theta_r)}{\sqrt{2\pi}\,\sigma(\psi_a - \psi)} \exp\left\{-\dfrac{\left[\ln\left(\frac{\psi_a}{\psi - \psi_a}\right) - \mu\right]^2}{2\sigma^2}\right\} & \psi < \psi_a \\[4mm] 0 & \psi \geqslant \psi_a \end{cases}$$

(23)

where ψ_a, which is related to r_{max} by Eq.(15), is the air-entry head. Differentiating Eq.(23) with respect to ψ and setting $g'(\psi) = 0$, the capillary pressure at the peak of $g(\psi)$, that is, the mode of $g(\psi)$, can be derived as function of ψ_a, σ, and μ:

$$\psi_0 = \psi_a[1 + \exp(-\mu - \sigma^2)]$$

(24)

where ψ_0 represents the mode of $g(\psi)$. Inverting Eq.(24) with respect to μ and substituting into Eq.(23) gives

$$g(\psi) = \begin{cases} \dfrac{(\theta_s - \theta_r)}{\sqrt{2\pi}\,\sigma(\psi_a - \psi)} \exp\left\{-\dfrac{\left[\ln\left(\frac{\psi_a - \psi}{\psi_a - \psi_0}\right) - \sigma^2\right]^2}{2\sigma^2}\right\} & \psi < \psi_a \\[4mm] 0 & \psi \geqslant \psi_a \end{cases}$$

(25)

The above equation has an alternative three-parameter lognormal distribution form because the distribution of

$$\ln\left(\frac{\psi_a - \psi}{\psi_a - \psi_0}\right),$$

(26)

obeys the normal distribution $\mathcal{N}(\sigma^2, \sigma^2)$. The mean $\bar{\psi}$, the median ψ_m, and the variance σ_ψ^2 of $g(\psi)$ are expressed by the following functions with respect to ψ_a, ψ_0, and σ.

$$\bar{\psi} = \psi_a - (\psi_a - \psi_0)\exp(3\sigma^2/2)$$

(27)

$$\psi_m = \psi_a - (\psi_a - \psi_0)\exp(\sigma^2) \tag{28}$$

$$\sigma_\psi^2 = (\psi_a - \psi_0)^2 \exp(3\sigma^2)[\exp(\sigma^2) - 1] \tag{29}$$

Substituting Eq.(25) into Eq.(20) and integrating yields an expression for water retention:

$$S_e = \begin{cases} \dfrac{1}{2}\mathrm{erfc}\left[\dfrac{\ln\left(\dfrac{\psi_a - \psi}{\psi_a - \psi_0}\right) - \sigma^2}{\sqrt{2}\,\sigma}\right] & \psi < \psi_a \\[2em] 1 & \psi \geqslant \psi_a \end{cases} \tag{30}$$

where erfc denotes the complementary error function. The above expression for the saturation degree can be expressed in an equivalent form as

$$S_e = \begin{cases} Q\left[\dfrac{\ln\dfrac{\psi_a - \psi}{\psi_a - \psi_0}}{\sigma} - \sigma\right] & \psi < \psi_a \\[2em] 1 & \psi \geqslant \psi_a \end{cases} \tag{31}$$

where Q is the complementary normal distribution function defined as

$$Q(x) = \int_x^\infty \frac{1}{\sqrt{2\pi}}\exp\left(-\frac{u^2}{2}\right)du \tag{32}$$

TWO–PARAMETER LOGNORMAL DISTRIBUTION MODEL Kosugi [50] suggested to apply a restriction to one the parameter of the retention model in order to derive an analytical expression for the relative hydraulic conductivity according to Mualem's model [72]. Setting $\psi_a = 0$, Eq.(25) and Eq.(30) become respectively

$$g(\psi) = \frac{\theta_s - \theta_r}{\sqrt{2\pi}\,\sigma(-\psi)}\exp\left\{-\frac{\left[\ln\left(\dfrac{\psi}{\psi_0}\right) - \sigma^2\right]^2}{2\sigma^2}\right\} \tag{33}$$

$$S_e = \frac{1}{2}\mathrm{erfc}\left[\frac{\ln\left(\dfrac{\psi}{\psi_0}\right) - \sigma^2}{\sqrt{2}\,\sigma}\right] = S_e = Q\left[\frac{\ln\left(\dfrac{\psi}{\psi_0}\right)}{\sigma} - \sigma\right] \tag{34}$$

and still produce acceptable matches with retention curves of soils which have no distinct air-entry head. The pore capillary distribution, Eq.(33) is still not symmetrical. Looking at the S_e-ψ, Fig.(9), ψ_0 corresponds to the capillary pressure at the inflection point, and the effective saturation is equal to
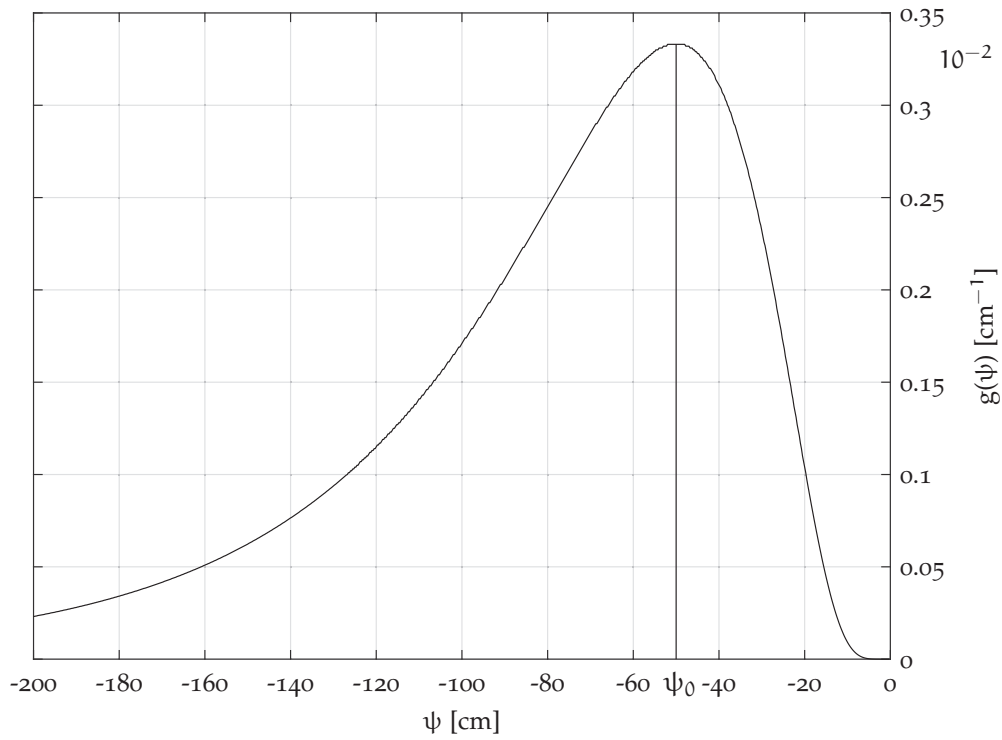
$$S_e(\psi_0) = Q(-\sigma) \tag{35}$$

Figure 8: Curve $g(\psi)$ - ψ with two-parameters lognormal distribution $\theta_s = 0.4$, $\theta_s = 0.1$, $\psi_0 = 50$[cm], $\psi_m = -71.7$[cm] [50].

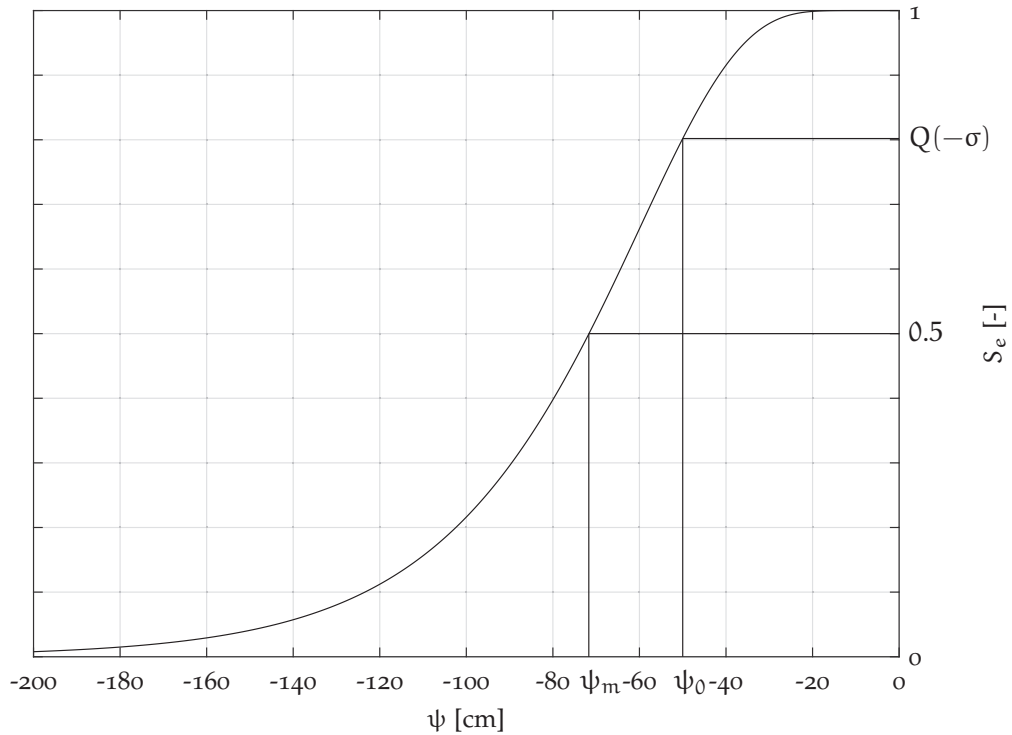**Figure 9:** Curve S_e - ψ with two-parameters lognormal distribution $\theta_s = 0.4$, $\theta_s = 0.1$, $\psi_0 = 50$[cm], $\psi_m = -71.7$[cm] [50].

Consequently, small σ value reduces $S_e(\psi_0)$ and makes the retention curve steep at the inflection point. The median, ψ_m, is given by substituting $S_e = 0.5$ into Eq.(34):

$$\psi_m = \psi_0 \exp(\sigma^2) \tag{36}$$

Inverting Eq.(36) with respect to ψ_0 and substituting into Eq.(33) and Eq.(34) yields

$$g(\psi) = \frac{\theta_s - \theta_r}{\sqrt{2\pi}\,\sigma(-\psi)} \exp\left\{ -\frac{\left[\ln\left(\frac{\psi}{\psi_m}\right)\right]^2}{2\sigma^2} \right\} \tag{37}$$

$$S_e = \frac{1}{2}\text{erfc}\left[\frac{\ln\left(\frac{\psi}{\psi_m}\right)}{\sigma}\right] = Q\left[\frac{\ln\left(\frac{\psi}{\psi_m}\right)}{\sigma}\right] \tag{38}$$

The capillary pressure distribution, Eq.(38), has the lognormal distribution from since the distribution of $\ln(-\psi)$ obeys the normal distribution $\mathcal{N}[\ln(-\psi_m), \sigma^2]$. Consequently, ψ_m, is identical to the geometric mean of $g(\psi)$.

Finally, it is possible to determine the pore radius distribution function $f(r)$ corresponding to the capillary pressure distribution Eq.(38) using the Young-Laplace equation, Eq.(15), and differentiating

$$f(r) = \frac{\theta_s - \theta_r}{\sqrt{2\pi}\,\sigma r} \exp\left\{ -\frac{\left[\ln\left(\frac{r}{r_m}\right)\right]^2}{2\sigma^2} \right\} \tag{39}$$

where r_m is the pore radius related to ψ_m by Young-Laplace equation.

To sum up, this model exhibits good fits as well as others emprical curve-fitting equations [52]. Furthermore, as pointed out above, the fact the parameters of this retention model have a physical significance on the θ-ψ curve and are related closely to the statistics of the pore radius distribution allows analyze problems connected to soil water conductivity, soil texture, hysteretic phenomena in water retention, spatial variability of soil hydraulic properties, and freezing/thawing processes.

3.2.5 Models for relative hydraulic conductivity

During his experiment with saturated columns of soil, Darcy introduced the hydraulic conductivity as a proportional factor between the pressure gradient and the specific discharge. The saturated hydraulic conductivity K_s has the dimension of a velocity, and it is defined as the unit of volume of a fluid crossing a unit area perpendicular to the flow in unit time per unit water-moving force. In a saturated medium the hydraulic conductivity depends both on the mechanical properties of the fluid, and the geometrical properties of the medium. Thus the saturated hydraulic conductivity can be expressed by the follow dimensional equation

$$K_s = Nd^2\nu^{-1} \tag{40}$$

where N is a dimensionless factor that takes into account of the shape of particles, d describes the soil's structure, and ν $[M(LT)^{-1}]$ is the dynamic

viscosity of the fluid.   Actually, in unsaturated soil the presence of air reduces the cross-sectional area of the water paths, and it is as if the soil's porosity was reduced up to the water content.

Let us define the relative hydraulic conductivity K_r as

$$K_r = \frac{K}{K_s} \tag{41}$$

where K is the unsaturated conductivity.   Following Mualem's work [72], based on pore size distribution, pore geometry, and connectivity, the relative hydraulic conductivity may be expressed by integrating the contributions of the individual pores according to Poiseulle's flow, thus one obtains

$$K_r(S_e) = S_e^{1/2} \left\{ \int_0^{S_e} \frac{dS_e}{|\psi|} \bigg/ \int_0^1 \frac{dS_e}{|\psi|} \right\}^2 \tag{42}$$

and finally the unsaturated hydraulic conductivity can be expressed as

$$K = K_s S_e^{1/2} \left\{ \int_0^{S_e} \frac{dS_e}{|\psi|} \bigg/ \int_0^1 \frac{dS_e}{|\psi|} \right\}^2 \tag{43}$$

BROOKS AND COREY   [82] substituting the Brooks and Corey soil water retention model, Eq.(9) in Eq.(42) one obtains:

$$K_r = S_e^{3 + 2/\lambda} \tag{44}$$

The combination of the water retention model expressed as Eq.(9) and the hydraulic conductivity model expressed as Eq.(44) is referred to as the Brooks and Corey model.

VAN GENUCHTEN   [102] substituting the Van Genuchten soil water retention model, Eq.(10) in Eq.(42) one obtains:

$$K_r = S_e^{1/2} [1 - (1 - S_e^{1/m})^m]^2 \tag{45}$$

The combination of the water retention model expressed as Eq.(10) and the hydraulic conductivity model expressed as Eq.(45) is referred to as the Brooks and Corey model.

TWO–PARAMETER LOGNORMAL DISTRIBUTION MODEL FOR RELATIVE HYDRAULIC CONDUCTIVITY   Combining Eq.(38) in Eq.(42) gives the functional relationship between K_r and S_e, and K_r and ψ [50]. The integral in Eq.(42) is transformed as follows:

$$\int_0^{S_e} \frac{dS_e}{|\psi|} = \frac{1}{\theta_s - \theta_r} \int_{\theta_r}^{\theta} \frac{d\theta}{|\psi|} = \frac{1}{\theta_s - \theta_r} \int_{-\infty}^{\Psi} \frac{1}{|\psi|} g(\psi) d\psi = \frac{1}{|A|(\theta_s - \theta_r)} \int_0^R r f(r) dr \tag{46}$$

When the pore-size distribution $f(r)$ is expressed as Eq.(39) the above integral becomes

$$\int_0^{S_e} \frac{dS_e}{|\psi|} = \frac{1}{|\psi_m|} \exp\left(\frac{\sigma^2}{2}\right) Q \left[\frac{\ln\left(\dfrac{\psi}{\psi_m}\right)}{\sigma} + \sigma \right] \tag{47}$$

Substituting $S_e = 1$ (that is, $\psi = 0$) into the above equation, one obtains

$$\int_0^1 \frac{dS_e}{|\psi|} = \frac{1}{|\psi_m|} \exp\left(\frac{\sigma^2}{2}\right) \tag{48}$$

and thus the relative hydraulic conductivity

$$K_r = S_e^{1/2} \left\{ Q\left[\frac{\ln\left(\frac{\psi}{\psi_m}\right)}{\sigma} + \sigma\right] \right\}^2 \tag{49}$$

Finally, substituting Eq.(38) into Eq.(49), K_r, can be expressed in the term of S_e or ψ:

$$K_r(S_e) = S_e^{1/2} \left\{ Q\left[Q^{-1}(S_e) + \sigma\right] \right\}^2 \tag{50}$$

$$K_r(\psi) = \left\{ Q\left[\frac{\ln\left(\frac{\psi}{\psi_m}\right)}{\sigma}\right] \right\}^{1/2} \left\{ Q\left[\frac{\ln\left(\frac{\psi}{\psi_m}\right)}{\sigma} + \sigma\right] \right\}^{1/2} \tag{51}$$

The combination of the water retention model expressed as Eq.(34) or Eq.(38) and the hydraulic conductivity model expressed as Eq.(50) and Eq.(51) is referred to as the lognormal distribution model.

3.2.6 Multimodal soil water retention function

So far, it has been shown how to obtain the soil water retention function and hence the hydraulic conductivity starting from the knowledge of the soil's pore-size distribution. Doing this, the soils is assumed to be unimodal, characterized by a single pore-size distribution function. In general soils exhibits multimodal pore-size distribution because of specific particle-size distributions or some genetic processes, both natural and artificial, that alter the soil's structure [20]. Therefore it is useful to take into account of this multimodality to better describe all those processes occur with in the soil. Othmer et al. [77], Durner [20], Ross and Smettem [88] proposed to describe the retention function of these type of soils by a multi-model function

$$S_e = \sum_{i=1}^N w_i S_{e,i}(\psi) \tag{52}$$

where N is the number of pores systems from which the total pore-size distribution is determined, and w_i is the weighting factor for each pore system i, subjected to the constrain that $0 < w_i < 1$ and $\sum w_i = 1$. As pointed out by Durner [20] unless the retention data are distinctly multimodal with little overlap of pore-size distribution, physically based parameters might loose their meaning and be considered curve-shape parameters only.

Whilst this approach allow to better describe the effect of multimodal pore-size distribution on the retention function, on the other hand the derivation of the unsaturated hydraulic conductivity requires a numerical evaluation of Eq.(42).

As pointed the reliability of the hydraulic conductivity model for multi-modal soil depends on the the assumption of isotropic organization of pores, the validity of the Poiseuille law for flow in large pores, the problem of air entrapment, and the problem of hysteresis [20].

3.2.7 Non isothermal water flow

So far it was assumed that the water flow is isothermal. According with Eq.(40) the hydraulic conductivity depends both on the water density and its viscosity. However, it is still not clear the relation between temperature and water flow since several soil-water flow parameters are influenced by it. The rate of change in μ with temperature is at least two order of magnitude greater than the rate of change in ρ with temperature. Consequently, at constant θ, changes in K related to temperature can be attributed solely to changes in ν with temperature. Constantz [15] proposed the follow expression to relate the unsaturated hydraulic conductivity and temperature:

$$K(T_2) = K(T_1)\frac{\nu(T_1)}{\nu(T_2)} \tag{53}$$

where T_1 is a reference temperature usually set to 293.15 [K] and $\nu(T_1) = 1002\,10^{-6}$ [Pa s]. Based on this equation, the value of K should increase by over three-fold between 5°C and 60°C.

According with Kestin et al.[48] in range $265.15 \leqslant T_2 \leqslant 4213.15$ the viscosity at a certain temperature T_2 may be expressed as

$$\ln\left[\frac{\nu(T_2)}{\nu(T_1)}\right] = \frac{-253.15 - T_1}{T_1 + 369.15}\left[1.2364 - 1.303\,10^{-3}(-253.15 - T_1)\right.$$
$$\left. + 3.6\,10^{-6}(-253.15 - T_1)^2 + 2.55\,10^{-8}(-253.15 - T_1)^3\right] \tag{54}$$

3.3 MASS CONSERVATION EQUATION

The mass conservation can be usefully represented using a Petri's net, as shown in Fig.(10). The mass conservation equation in a control volume
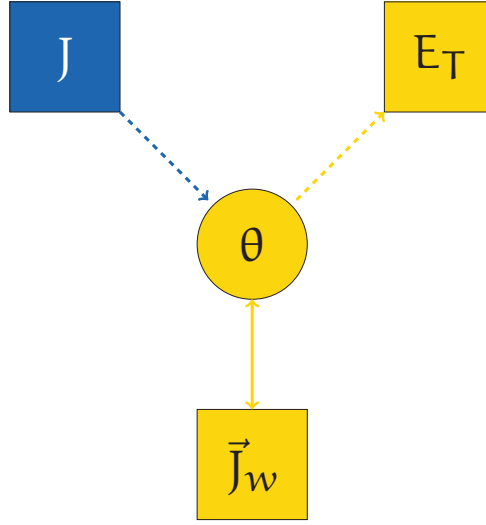

Figure 10: Assume for now there is no accumulation of water on the surface. The water content θ in the soil volume is determined by the water flux $\vec{J}_w$, the rate of precipitation J (input), and the rate of evapotranspiration E_T (outputs).

Symbol	Name
J	Precipitation rate
E_T	Evaporation
$\vec{J}_w$	Water flux

Table 1: Definitions of mass conservation terms

may be written as

$$\rho_w \frac{\partial \theta_w}{\partial t} = -\rho_w \nabla \cdot \vec{J}_w \tag{55}$$

The water flux $\vec{J}_w$ is modeled according to Darcy Buckingham's law

$$\vec{J}_w = -K(\psi)\vec{\nabla}(\psi + z) \tag{56}$$

where $K(\psi)$ is the hydraulic conductivity that depends on the liquid water saturation degree, and z is the vertical coordinate assumed positive upward. Eq.(133) has to be coupled with two closure equations one relating the water content and suction (see Sec.(3.2.4)), the other one for hydraulic conductivity and water content (see Sec.(3.2.5)).

The boundary conditions at the ground surface are specified by prescribing precipitation J, and the evapotranspitation, E_T. The boundary condition at the bottom of the domain is specified by prescribing the water flow, $\vec{J}_w$.

3.4 THE SOIL ENERGY CONTENT

The energy content $\mathcal{E}$ of the soil volume V_c is

$$\mathcal{E} = U + E_k + E_p \tag{57}$$

where U is the internal energy, E_k the kinetic energy, and E_p the potential energy. Studying the water flow in soils the kinetic energy may be neglected since the water velocities are small.

The internal energy, neglecting the energy of air, can be calculated as the sum of the internal energy of the soil particles, and water:

$$U = U_s + U_w \tag{58}$$

hence

$$U = H_s + h_w M_w \tag{59}$$

where H_s, h_w are respectively the enthalpy of the soil particles, and the specific enthalpy of water. The specific enthalpy of water can be calculated as

$$\int h_w \, dT = h_w{}^\circ + c_w (T - T_{ref}) \tag{60}$$

where $h_w\check{r}$ is the specific enthalpy of water at reference temperature T_{ref}, c_w is the specific thermal capacity of water. In the same manner for ice, one obtains

$$\int h_i \, dT = h_i{}^\circ + c_i (T - T_{ref}) \tag{61}$$

where $h_i\check{r}$ is a the specific enthalpy of ice at reference temperature T_{ref}, c_i is the specific thermal capacity of ice. The difference

$$h_w{}^\circ - h_i{}^\circ = l \tag{62}$$

equals the latent heat of fusion. Eventually, posing $T_{ref} = T_m$ and $h_i{}^\circ = 0$, the enthalpy of water becomes:

$$H_w = M_w L + M_w c_w (T - T_m) = \rho_w V_w l + \rho_w V_w c_w (T - T_m) \tag{63}$$

Finally, Eq.(58) can be written as

$$U = \rho_s V_s c_s (T - T_m) + \rho_w V_w l + \rho_w V_w c_w (T - T_m) \tag{64}$$

Dividing Eq.(64) by the soil volume V_c one obtains the internal energy per unit volume

$$u = u_s + u_{sp} = \rho_s c_s (T - T_{ref})(1 - \theta_s) + \rho_w [l + c_w (T - T_{ref})]\theta_w \tag{65}$$

The potential energy of the volume V_c is calculated as the potential energy of just water since it is assumed that soil particles can not move:

$$E_p = E_{p,w} \tag{66}$$

Thus the potential energy for a unit volume of soil can be written as

$$E_p = \rho_w V_w g z \tag{67}$$

and dividing by the soil volume V_c one obtains

$$e_p = \rho_w \theta_w g z \tag{68}$$

which represents the potential energy per unit volume.

3.5 ENERGY CONSERVATION EQUATION

The energy conservation may be usefully represented using a Petri net, as shown in Fig.(11). The energy conservation in a control volume may be
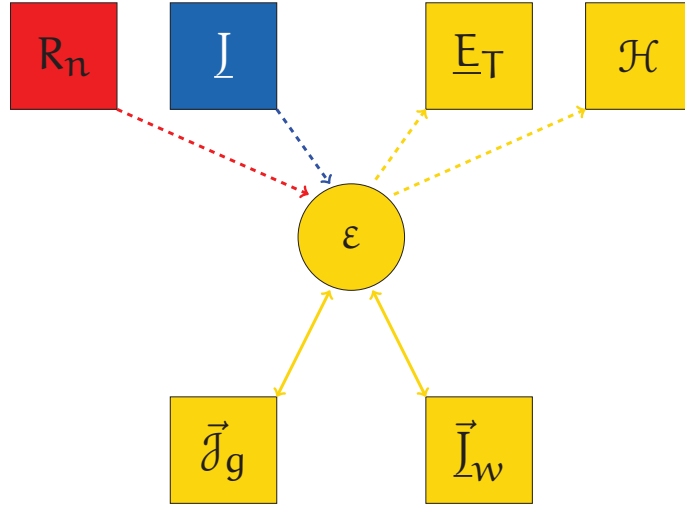

Figure 11: The variation in time of the internal energy per unit volume ε results from the balance of the heat fluxes within the soil and at the ground surface.

Symbol	Name
J	Heat flux due to precipitation
$\underline{E}_T$	Evaporation heat flux
$\vec{J}_w$	Heat advected by flowing water
$\vec{J}_g$	Conduction flux
R_n	Net radiation
$\mathcal{H}$	Sensible heat
ε	Energy per unit volume

Table 2: Definition for energy conservation terms

described as

$$\frac{\partial}{\partial t}(\varepsilon) = \frac{\partial}{\partial t}(u + e_p) = -\nabla \cdot (\vec{J}_w + \vec{J}_g) \tag{69}$$

where:

- $\vec{J}_g$ is the conduction flux, accorging to Fourier's law, may be written as

$$\vec{J}_g = -\lambda \vec{\nabla} T \tag{70}$$

where λ is the thermal conductivity of the soil that depends on the thermal conductivity of soil particles, and on the water content [17].

- $\vec{J}_\theta$ is the heat advected by flowing water, and may be written as

$$\vec{J}_w = \rho_w[l + c_w(T - T_m)]\vec{J}_w \tag{71}$$

The boundary condition at the ground surface are specified by prescribing the net radiation R_n, and the heat fluxes due to the precipitation, $\underline{J}$, evapotranspitation, $\underline{E}_T$, and the sensible heat $\mathcal{H}$.

The boundary condition at the bottom of the domain are specified by prescribing both the conduction flux, $\vec{\jmath}_g$, and the heat advected by flowing water, $\vec{J}_w$.

Deriving the right hand side of Eq.(69) one obtains

$$\frac{\partial}{\partial t}(u + e_p) = [\rho_s(1 - \theta_s)c_s + \rho_w\theta_w c_w]\frac{\partial T}{\partial t}$$
$$+ \rho_w [l + c_w(T - T_m) + gz]\frac{\partial\theta_w}{\partial t} \quad (72)$$

Let us define

$$C_T := \rho_s c_s(1 - \theta_s) + \rho_w\theta_w c_w \quad (73)$$

the total thermal capacity of the soil volume. As we can see in Eq.(72), the variation in time of the total energy may be seen as the sum of three contributes: the first term of the right hand side is the sensible part and takes into account of the variation of temperature in time, whilst the second one takes into account of the variation of the water content.

Substituting Eq.(72) and Eq.(73) into Eq.(69) gives the following equation

$$C_T\frac{\partial T}{\partial t} + \rho_w [l + c_w(T - T_m) + gz]\frac{\partial\theta_w}{\partial t} = -\nabla \cdot (\vec{J}_w + \vec{\jmath}_g) \quad (74)$$

Using Eq.(55) in Eq.(74) gives

$$C_T\frac{\partial T}{\partial t} + \rho_w [l + c_w(T - T_m) + gz]\left(-\nabla \cdot \vec{J}_w\right) = -\nabla \cdot (\vec{J}_w + \vec{\jmath}_g) \quad (75)$$

Finally the energy conservation can be written as

$$C_T\frac{\partial T}{\partial t} + \rho_w c_w\vec{J}_w \cdot \vec{\nabla}T + \rho_w gz\nabla \cdot \vec{J}_w - \nabla \cdot \vec{\jmath}_g = 0 \quad (76)$$

4 | PHYSICS AND EQUATIONS OF WATER IN FREEZING SOILS

4.1 ASSUMPTION OF THE FREEZING SOILS MODEL

The purpose of this model is to study the thermal and hydrological effects of freezing-thawing processes in saturated and unsaturated soils. This mathematical model is based on the following assumptions [16]:

- rigid soil scheme, i.e. the volume V_c is constant and no volume expansion during freezing is allowed. Therefore the density of water ρ_w and of ice ρ_i must be considered equal, because otherwise the change of the water density upon freezing would lead to unrealistically large gauge pressures that cannot be converted into an expansion of the soil matrix, due to the lack of mechanical model.

- The *freezing=drying* assumption [68] implies that: (i) the freezing (thawing) water is like evaporating (condensing) water; (ii) the ice pressure is equal to the air pressure; (iii) the water and ice content in the soil may be related to the soil matric potential according to the water retention curve; (iv) the volume V_c is representative of soil volumes above the water table or at shallow depths below the water table, where the water pressure may be considered similar to the atmospheric pressure.

- The phase change is assumed to occur at the thermodynamic equilibrium and the ice seeding and its growing is not taken into

As underlined in the first chapter, whilst the introduction of some assumptions allow to provide answer to well-posed questions with some degree of approximation [54], it could not able to look upon complexity of the entire processes involved in the frozen ground. Therefore, let us briefly remark the above assumption.

Firstly, the rigid soil scheme assumption, and that comes with it, is a significant easing the study of soil freezing-thawing. It is worthwhile to stress that is strong when a soil containing water freezes, it may expand much more than one would predict from the expansion due to the freezing of water that is in the soil [40]. This is expansion is commonly named as frost heave. It is worthwhile to stress that right the engineering aspect of frost heave [40] boosted in part the development of freezing-thawing model [54]. However, since the purpose of this model is not to simulate the freezing-induced soil deformation this assumption does not seem to be too much limiting, but rather allow not to provide a soil mechanical model.

About the *freezing=drying*, most authors have not a clear view of the motivations behind it. Spaans and Baker [95] wrote: "the broad assumption of zero gauge pressure in the ice phase has been questioned under certain condition [69] [70], but thus far there is scant evidence against it, except

in obvious cases (heaving)". Also Hansson [31] advance doubt on the *freezing=drying* assumption: "Usually in soil science the ice pressure is sometimes assumed to equal the zero gauge pressure, with the reference pressure being atmospheric. While this assumption has often been debated, no consensus has yet been reached. In particular, if a soil is unsaturated the potential of heaving is reduced such that the assumption of zero ice pressure is more likely to hold". Even though a compelling physical motivation still misses, this assumption is widely used in literature. Firstly it allows to simplify the Young-Laplace equation (see Sec.(3.1)). Secondly, if the ice is regarded as an air bubble, the water flow in it may be studied with an unsaturated flow theory.

Freezing and thawing processes may not always occur at thermodynamic equilibrium [54]. Disequilibrium phase change can occur at the onset of soil freezing because temperatures can decrease more rapidly than equilibrium ice formation. The possibility of disequilibrium states should not be neglected if the rate of temperature changes exceeds $0.1°Ch^{-1}$ in the range of 0°C to −0.5°C. Furthermore, neglecting the kinetic of the phase change allow to assume that the melting temperature and the freezing temperature are the same even though the freezing/thawing processes may occur at different temperatures. Actually, all molecules in a liquid undergo Brownian motion. For freezing to occur in a supercooled liquid, the diffusing molecules must spontaneously form a small cluster (called a nucleus or embryo) of molecules which has a transient structure similar to that of ice. In a supercooled liquid such clusters form and dissipate rapidly. If however the cluster is larger than some critical size, it becomes energetically favourable for other diffusing molecules to join the structure, and it grows through the sample [109]. Thus it is possible to cool water below the melting temperature without it turns into ice (metastable state), whilst it is not possible to maintain water in solid state at a temperature slightly above the melting point unless it stars thawing.

4.2 YOUNG–LAPLACE EQUATION

The derivation of the Young-Laplace equation in presence of ice will be performed following Dall'Amico's work [17].

Assuming that the same relation applies for water-air and water-ice interface, one obtains:

$$\begin{cases} p_w = p_a - \gamma_{aw}\dfrac{\partial A_{aw}()}{V_w} = p_a - p_{aw}(r) \\ p_w = p_i - 2\gamma_{iw}\dfrac{\partial A_{iw}()}{\partial V_w} p_i - p_{iw}(r) \end{cases} \tag{77}$$

Let us suppose an unsaturated soil where the water invades the pores having menisci of radius $r \leqslant R$. Accordingly with Young-Laplace's equation, the water pressure at the macroscale is

$$p_{w0} = p_a - \gamma_{aw}\frac{\partial A_{aw}(r_0)}{V_w} = p_a - p_{aw}(R) \tag{78}$$

where p_{w0} is the water negative pressure due to the menisci surfaces created by the water-air interface in the pores with radius $r < R$.

Let us suppose to freeze some water in the soil: this means that the water-air interface present at R is replaced by an ice-air interface, and that a new ice-water interface is created at a smaller radius r. Consequently the water in the capillary of radius r will be subject to a new pressure p_{w1}, and the ice will be subject to the pressure p_i. Hence one obtains:

$$\begin{cases} p_{w1} = p_i - \gamma_{iw}\dfrac{\partial A_{iw}(r)}{V_w} := p_i - p_{iw}(r) \\ p_i = p_a - \gamma_{ai}\dfrac{\partial A_{ai}(R)}{V_w} := p_a - p_{ai}(R) \end{cases} \tag{79}$$

This implies:

$$p_{w1} = p_a - \gamma_{ai}\frac{\partial A_{ai}(R)}{V_w} - \gamma_{iw}\frac{\partial A_{iw}(r)}{V_w} \tag{80}$$

In agreement with the assumption *freezing=drying*, we should think that the ice in the capillary behaves like air, i.e. the water below receives an increment in negative pressure (suction) as if the water was evaporated or drained. In this case the water pressure p_{w1} would be the same as no ice would be present, and the ice pressure is equal to air pressure. Thus this hypothesis implies that

$$p_{w1} = p_a - p_{aw}(r) \tag{81}$$

$$p_i = p_a - p_{ia}(R) \equiv p_a \tag{82}$$

which means that the interface pressure ice-water is equal to the interface pressure air-water and that the interface pressure ice-air is zero if the pressure gauge of air is taken to be null. Therefore from the assumption *freezing=drying* and the capillary representation, straightly derives that ice phase has a "zero-gauge" pressure.

4.3 FREEZING POINT DEPRESSION

The phase change of pure water at atmospheric pressure occurs in a simple switching mechanism when the melting temperature, $T_m = 273.15$ K, is crossed. Instead the water in soil pores freezes-thaws over a range of temperatures that can be several degrees below the melting temperature. This is the consequence of both the presence of solutes and the effect of capillary and absorptive forces that attract liquid water to the soil pore apertures and soil particles, respectively. Thus at equilibrium, considering an unsaturated volume of soil at a certain temperature below T_m water and ice will coexist since the melting temperature may differ in each point of the volume accordingly to the concentration of solutes and capillary absorptive forces.

4.3.1 The Gibbs–Thomson equation

The derivation of the Gibbs-Thomson equation will be performed following Dall'Amico's Doctoral Thesis [17] and Acker's work [2].

The thermodynamic equilibrium of retained water and ice in soil can be studied considering the equilibrium of an aqueous solution in a capillary tube. Since in a capillary tube the surface-to-volume ratio is small the internal energy associated to the interface can not be neglected. As proposed by Safran [90] interfaces should be better treated as phases by themselves, where the surface energy plays the role of pressure, and area plays the role of volume. The total variation of the internal energy for each phase is

$$\begin{cases} dU_w(T,p,M) = T_w \, dS_w() - p_w \, dV_w() + \mu_w() \, dM_w \\ dU_i(T,p,M) = T_i \, dS_i() - p_i \, dV_i() + \mu_i() \, dM_i \\ dU_{iw}(T,p,M) = \gamma_{iw} \dfrac{\partial A_{iw}()}{\partial V_w} \, dV_w() \end{cases} \quad (83)$$

where T, p, M, S, V, μ, A_{iw} are the temperature, pressure, mass, entropy, volume, chemical potential of the phases, and A_{iw} the area of the interface. The parenthesis make clear which are the independent variables and which are the dependent ones. In a closed system $dU = 0$, thus:

$$dU_w() + dU_i() + dU_{iw} = 0 \quad (84)$$

which means that

$$dU_w() + dU_{iw}() := dU_w^*() = -dU_i() \quad (85)$$

$$T_w \, dS_w() - \left(p_w + \gamma_{iw} \frac{\partial A_{iw}()}{\partial V_w} \right) dV_w() + \mu_w() \, dM_w =$$
$$- T_i \, dS_i() + p_i \, dV_i() + \mu_i() \, dM_i \quad (86)$$

At the equilibrium the entropy of a closed system tends to a maximum:

$$dS(U,V,M) = 0 \quad (87)$$

hence, considering that $dM_w = -dM_i$, $dV_w = dV_i$, and that $dS = dS_w + dS_i$ one obtains

$$dS() = \left(\frac{1}{T_w} - \frac{1}{T_i}\right) dU_w() + \left(\frac{p_w + \gamma_{iw}\frac{\partial A_{iw}()}{\partial V_w}}{T_w} - \frac{p_i}{T_i}\right) dV_w$$

$$- \left(\frac{\mu_w()}{T_w} - \frac{\mu_i()}{T_i}\right) dM_w = 0 \quad (88)$$

The co-existence of solid and liquid phases under varying thermodynamic conditions in a capillary tube requires:

$$T_i = T_w \tag{89a}$$

$$p_i = p_w + \gamma_{iw}\frac{\partial A_{iw}()}{\partial V_w} \tag{89b}$$

$$\mu_i = \mu_w \tag{89c}$$

namely the thermal equilibrium, Eq.(89a), the mechanical equilibrium, Eq.(89b), and the chemical equilibrium, Eq.(89c).

When an aqueous solution freezes, the ice is nearly pure, and the remaining unfrozen water is the solvent for all of the solutes, at concentrations that become very large as temperature falls [109]. Consequently, the chemical potential of liquid water is modified by the osmotic pressure whilst the ice does not. It is also assumed that the liquid phase is incompressible, and the specific entropy is constant over the temperature range of interest. Thus the chemical potential of the liquid water can be written as:

$$\mu_w(T_w, p_w, x) = \mu^\circ(T_m, p_a) + v_w(p_w - p_a) + s_w(T_m - T_w) - v_w\pi_w(T_w, x) \tag{90}$$

where μ° is the chemical potential of pure water at the planar melting point T_m and atmospheric pressure p_a, v_w is the specific volume of water, s_w the specific entropy of pure water at standard pressure and temperature; π_w is the osmotic pressure of the solution and x is the solute mole fraction in the liquid. It is assumed that the osmotic pressure of the solution is only a function of temperature and mole fraction of the solute.

Furthermore, let us assume that there are no nonisotropic stresses on the ice, that the ice is incompressible, and that over the temperature range of interest, the specific entropy of the ice is independent of temperature, then the chemical potential of ice can be written:

$$\mu_i(T_i, p_i) = \mu^\circ(T_m, p_a) + v_i(p_i - p_a) + s_i(T_m - T_i) \tag{91}$$

where v_i is the specific volume of ice, s_i the specific entropy of ice at standard pressure and temperature. As Eq.(89c) Eq.(89a) establish, thus

$$v_w(p_w - p_a) + s_w(T_m - T^*) - v_w\pi_w(T^*, x) = v_i(p_i - p_a) + s_i(T_m - T^*) \tag{92}$$

where T^* is the temperature at the equilibrium. According with the *freezing=drying* assumption, the mechanical equilibrium at the ice-water interface is not fulfilled and Eq.(89b) turns in

$$p_a - p_w = \gamma_{aw}\frac{\partial A_{aw}}{\partial V_w} \tag{93}$$

Combining the above equation and Eq.(92) one obtains

$$T_m - T^* = \frac{\gamma_{aw}\nu_w}{(s_w - s_i)}\frac{\partial A_{aw}}{\partial V_w} + \frac{\nu_w\pi_w}{(s_w - s_i)} \tag{94}$$

Given the definition of the specific enthalpy:

$$dh = T ds \tag{95}$$

and considering that the phase change occurs at constant pressure and temperature, on obtains

$$s_w - s_i = \frac{1}{T_m}\int_i^w dh = \frac{l}{T_m} \tag{96}$$

where l is the specific latent heat of fusion. Substituting Eq.(96) into Eq.(94) gives the following equation

$$\Delta T = T_m - T^* = \frac{\gamma_{aw}\nu_w T_m}{l}\frac{\partial A_{wa}}{\partial V_w} + \frac{\nu_w\pi_w T_m}{l} \tag{97}$$

that allow to know the freezing point depression ΔT once the capillary radius r and the osmotic pressure of the solution π_w are known.

Furthermore the above equation can be written as

$$\Delta T = \frac{2\gamma_{aw}\nu_w T_m \cos\alpha}{l\,r} + \frac{\nu_w\pi_w T_m}{l} \tag{98}$$

4.4 WATER AND ICE IN SOILS

4.4.1 The volume conservation

Let us consider a rigid control volume of soil V_c. Generally it is a composite of four different constituents, Fig.(12),: (i) soil particles, (ii) ice, (iii) liquid water, (iv) and gas or air. The volume conservation requires:
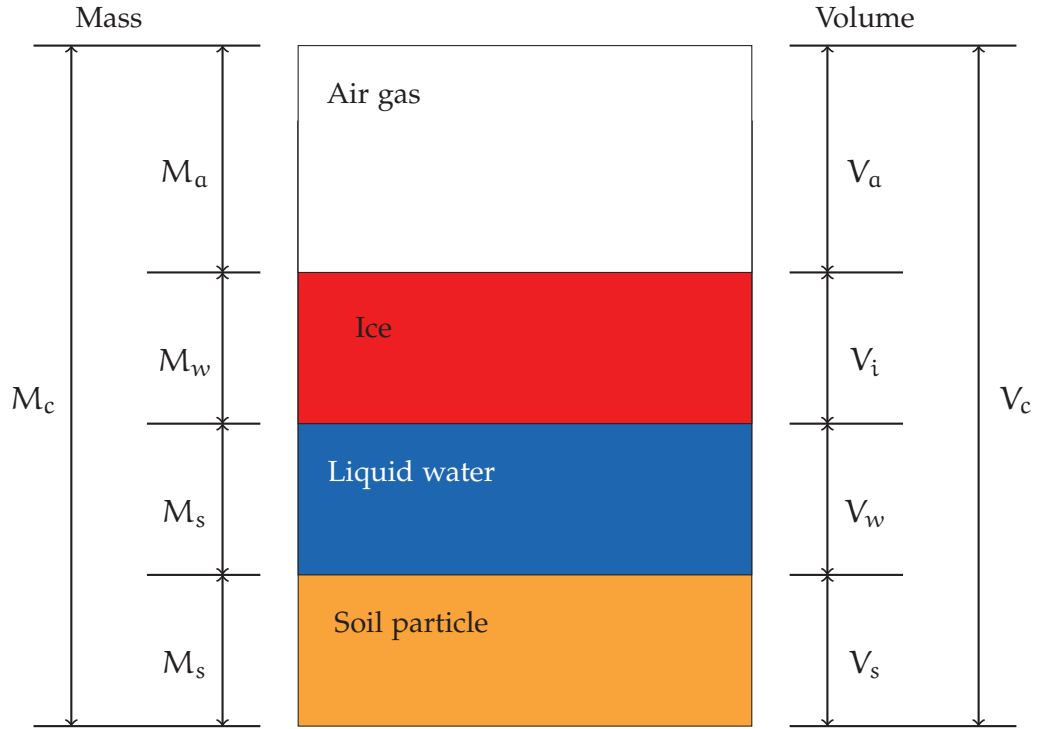

Figure 12: Frozen soil constituents and schematization of the control volume V_c [80].

$$V_s + V_i + V_w + V_a = V_s + V_{voids} = V_c \tag{99}$$

Let us define:

$$\theta_i := \frac{V_i}{V_c} \tag{100}$$

the adimensional and ice content.

It is usefull to introduce the total water volume in the soil as

$$V_{tot} = V_w + V_i \tag{101}$$

hence

$$\theta := \frac{V_{tot}}{V_c} = \theta_w + \theta_i \tag{102}$$

The total water content has to satisfy the follow restriction:

$$0 \leqslant \theta_r \leqslant \theta \leqslant \theta_s \leqslant 1 \tag{103}$$

where θ_r and θ_s are respectively the residual water content and the water content at saturation that corresponds to the soil porosity.

It is worthwhile to underline that during the phase change of water the mass is conserved and not the volume because of the different density of water and ice, thus:

$$dM_w + dM_i = 0 \tag{104}$$

4.4.2 Model for soil water retention

Because of capillary effects and dissolved salt there will be a range of depressed melting point over which the soil will freeze, therefore also freezing is a selective process (see Sec(4.3)). So far only capillary effect will be considered. From Gibbs-Thomson equation Eq.(94) it is possible to determine the radius at which occurs the water-ice interface for each temperature:

$$\hat{r}(T) := -\frac{2\gamma_{aw}v_w T_m \cos\alpha}{l(T - T_m)} \quad \text{for } T < T_m \tag{105}$$

At $T = T_m$ the water-ice interface is flat, i.e. $r \to \infty$.

It should be emphasized that $\hat{r}$ depends just on temperature and define the pore-size at which the water-ice interface occurs. Let us assume that water occupies pores with radius up to R and temperature drops below T_m. Looking at Fig.(13), since $\hat{r} < R$ liquid water will be confined in pores with radius smaller than $\hat{r}$, while between $\hat{r}$ and R ice will form. If some water will be added to the system it will turn into ice.

On the other hand, in Fig.(14) $\hat{r}$ is greater than R thus the entire water content is in the liquid phase. Whereby ice forms, it will be necessary to add water up to $\hat{r}$, otherwise the added water will remain in liquid phase.

The knowledge of the radius at which the ice-water interface occurs at each temperature below the melting point, allows to easily extends the two-parameter lognormal distribution model for soil water retention [50] also to the frozen soil in order to determine the water and ice content. Therefore, as well the water content was defined as Eq.(13), it is possible to introduce the following definitions for the liquid water content

$$\theta_w = \theta_r + \int_0^{\hat{r}} f(r)\,dr \tag{106}$$

and for the ice content

$$\theta_i = \int_{\hat{r}}^R f(r)\,dr \tag{107}$$

where $f(r)$ is the pore radius distribution function, Eq.(39), corresponding to the two-parameter lognormal distribution model for soil water retention, Eq.(38). Furthermore we can notice that in the first case, Fig.(13), at $\hat{r}$ the water-ice interface really occurs, whilst in the second one, Fig.(14), $\hat{r}$ identifies a "potential" water-ice interface since there is no enough water for ice forming. Thus to make the definitions of both the water and the ice content, Eq.(106) Eq.(107), consistently with the physics of the problem it is necessary to introduce the following definition

$$r^*(R, T) = \begin{cases} R & \text{if } \hat{r} \geqslant R \quad \text{or } T \geqslant T_m \\ \hat{r} = -\dfrac{2\gamma_{aw}v_w T_m \cos\alpha}{l(T - T_m)} & \text{otherwise} \end{cases} \tag{108}$$

Thus one obtains

$$\theta_w = \theta_r + \int_0^{r^*} f(r)\,dr \tag{109}$$

and

$$\theta_i = \int_{r^*}^R f(r)\,dr \tag{110}$$

To better clarify the meaning of Eq.(108) it is worthwhile to look again at Fig.(13) and Fig.(14). In Fig.(13), according with Eq.(108) the water-ice interface r^* is set to coincides with $\hat{r}$ and therefore Eq.(109) and Eq.(110) becomes respectively

$$\theta_w = \theta_r + \int_0^{r^*} f(r)\,dr \qquad \theta_i = \int_{r^*}^R f(r)\,dr \tag{111}$$

consistently with the fact that both the water and ice occur.

Conversely in Fig.(14), according with Eq.(108) the water-ice interface r^* is set to coincides with R and therefore Eq.(109) and Eq.(110) becomes respectively

$$\theta_w = \theta_r + \int_0^R f(r)\,dr \qquad \theta_i = \int_R^R f(r)\,dr = 0 \tag{112}$$
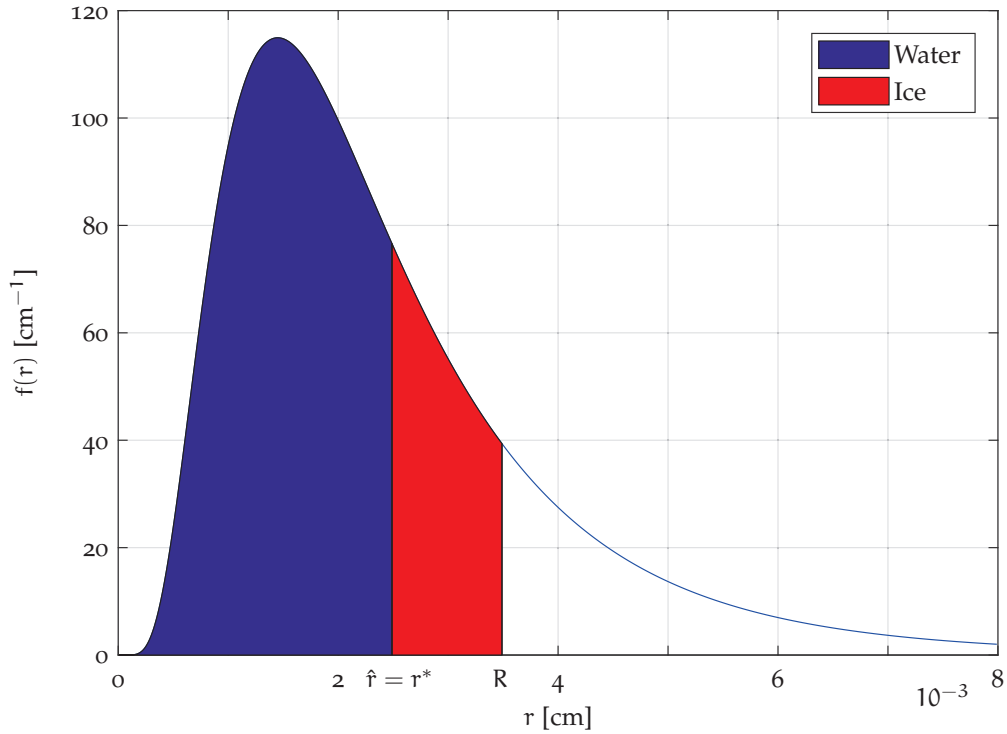
consistently with the state of the system.

Figure 13: The pore-size distribution is described by a two-parameters lognormal distribution [50] for $\theta_s = 0.4$, $\theta_r = 0.1$, $\sigma = 0.6$, $r_m = 2.1\,10^{-3}$[cm]. Let us assume that $\rho_w = \rho_i$. According with Eq.(108) water in pores with radius smaller than r^* remains liquid, whilst that in pores with radius $r^* \leqslant r \leqslant R$ turns into ice.

According with Kosugi's water retention model we have that

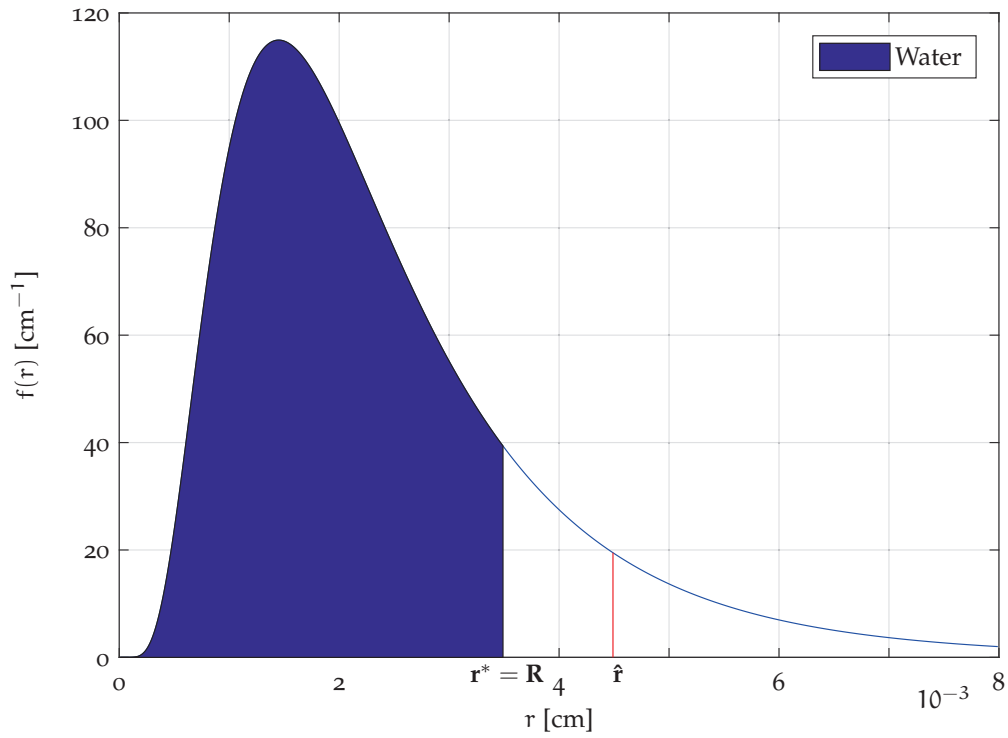$$g(\psi) = f(r(\psi))\frac{dr}{d\psi} \tag{113}$$

Figure 14: The pore-size distribution is described by a two-parameters lognormal distribution [50] for $\theta_s = 0.4$, $\theta_r = 0.1$, $\sigma = 0.6$, $r_m = 2.1\,10^{-3}$[cm]. Since $\hat{r} > R$ the entire water does not freeze and according with Eq.(108) it has to be set $r^* = \hat{r}$.

and hence the water content and the ice content may be expressed as

$$\theta_w = \theta_r + \int_{-\infty}^{\psi^*} g(\psi)d\psi \qquad \theta_i = \int_{\psi^*}^{\Psi} g(\psi)d\psi \tag{114}$$

where Ψ is related to R by Eq.(3), and according with Eq.(108) ψ^* is defined as:

$$\psi^*(\Psi, T) = \begin{cases} \Psi & \text{if } \hat{r} \geqslant -\dfrac{2\gamma_{aw}\cos\alpha}{\rho_w g\,\Psi} \text{ or } T \geqslant T_m \\ \hat{\psi} = \psi(\hat{r}) = \dfrac{l(T - T_m)}{g\,T_m} & \text{otherwise} \end{cases} \tag{115}$$

4.4.3 The phase transition

As seen in Sec.(3.2.4) the water content can be written as

$$\theta_w = \theta_r + \int_0^{r^*} f(r)dr \tag{116}$$

whilst the ice content

$$\theta_i = \int_{r^*}^{R} f(r)dr \tag{117}$$

Neglecting water flux, during freezing/thawing processes the mass of the system must be conserved:

$$\rho_w\theta = \rho_w\theta_w + \rho_i\theta_i \tag{118}$$

hence

$$\rho_w \left(\theta_r + \int_0^R f(r)\,dr \right) = \rho_w \left(\theta_r + \int_0^{r^*} f(r)\,dr \right) + \rho_i \int_{r^*}^R f(r)\,dr \qquad (119)$$

the left hand side term is the total water mass, on the right hand side the first term is the unfrozen water mass and the second one is the ice mass.

Assuming that both the water and the ice density are time independent, the time derivative of Eq.(119) is:

$$\rho_w \frac{\partial}{\partial t} \int_0^R f(r)\,dr = \rho_w \frac{\partial}{\partial t} \int_0^{r^*} f(r)\,dr + \rho_i \frac{\partial}{\partial t} \int_{r^*}^R f(r)\,dr \qquad (120)$$

Expanding time derivatives in the right hand side term one obtains

$$\rho_w \frac{\partial}{\partial t} \int_0^R f(r)\,dr = \rho_w \frac{\partial r^*}{\partial t} f(r^*) + \rho_i \left(\frac{\partial R}{\partial t} f(R) - \frac{\partial r^*}{\partial t} f(r^*) \right) \qquad (121)$$

According to the definition of r^*, Eq.(108), its time derivative becomes

$$\frac{\partial r^*}{\partial t} = \begin{cases} \dfrac{\partial R}{\partial t} & \text{if } \hat{r} \geqslant R \text{ or } T \geqslant T_m \\[2mm] \dfrac{\partial \hat{r}}{\partial t} = \dfrac{2\gamma_{aw} v_w T_m \cos\alpha}{(T - T_m)^2} \dfrac{\partial T}{\partial t} & \text{otherwise} \end{cases} \qquad (122)$$

From Eq.(122) it is clear how when the temperature increases, $\partial T/\partial t > 0$, also $\hat{r}$ will increase, $\partial \hat{r}/\partial t > 0$. As a consequence, $\hat{r}$ moves towards R and these leads to ice content decreasing, consistently with the thawing process ($\partial T/\partial t > 0$). On freezing the contrary is also true: while temperature drops $\hat{r}$ becomes smaller and smaller and the ice content increases.

Therefore the phase transition from water to ice (or vice versa) can be easily obtain deriving respect to time Eq.(110)

$$\frac{\partial \theta_i}{\partial t} = \frac{\partial R}{\partial t} f(R) - \frac{\partial r^*}{\partial t} f(r^*) \qquad (123)$$

This equation states that the variation in time of the ice content is due to the contribution of two terms. The first term on the right hand side takes into account of the variation of θ_i due to the variation of the total water content. To better clarify, let us suppose that $r^* < R$ and r^* does not vary in time, i.e. $\partial T/\partial t = 0$. Hence if water is added according to Mualem's assumption, pores with radius larger than R will be fulfilled, i.e. $\partial R/\partial t > 0$. Consequently the added water turns into ice, Fig(15). The contrary is also true. Thus we can observe a variation of the ice content at constant temperature just because there is a variation of the total water content.

Regarding the second term, it takes into account of the variation of the ice content due to the variation of r^* i.e. of temperature. Likewise before, assuming that $r^* < R$ and that R does not vary in time, i.e. the total water content is constant in time. Let us suppose to cool the soil sample i.e. $\partial T/\partial t < 0$, hence according with Eq.(122) $\partial r^*/\partial t < 0$. This means that water freezes and thus $\partial \theta_i/\partial t > 0$, Fig(16). On the contrary warming ($\partial T/\partial t > 0$) yields to have $\partial r^*/\partial t > 0$ and consequently $\partial \theta_i/\partial t < 0$.
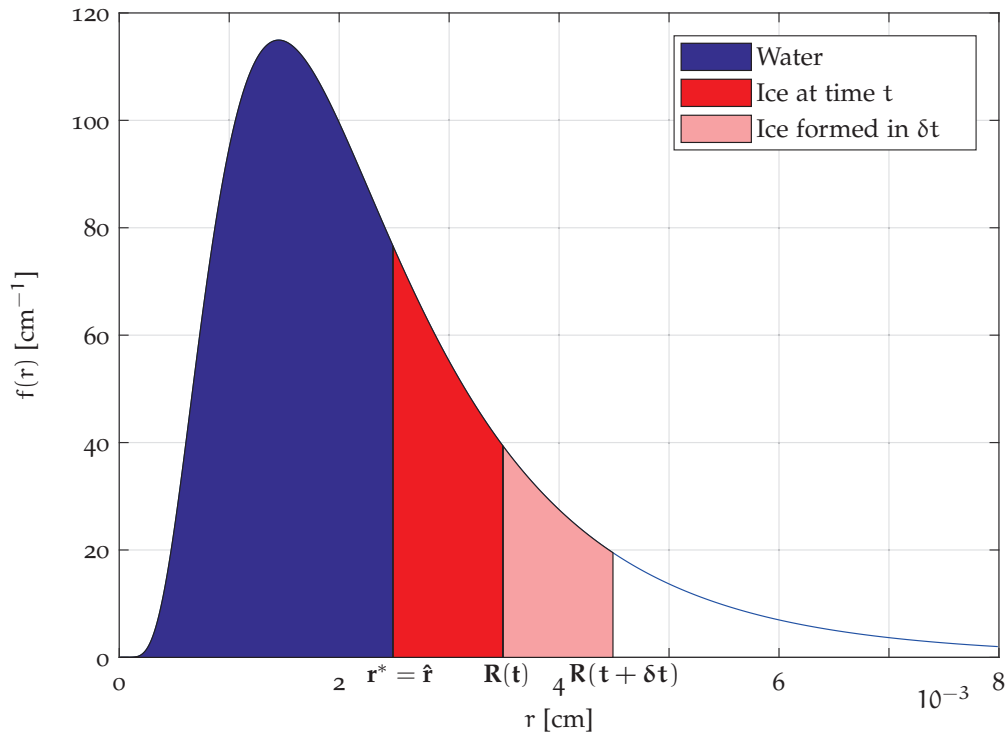
Figure 15: Let us assume that $r^* < R$ and r^* does not vary in time, i.e. $\partial T/\partial t = 0$. Additionally let us assume that $\rho_w = \rho_i$. The added water in the time δt turns into ice.
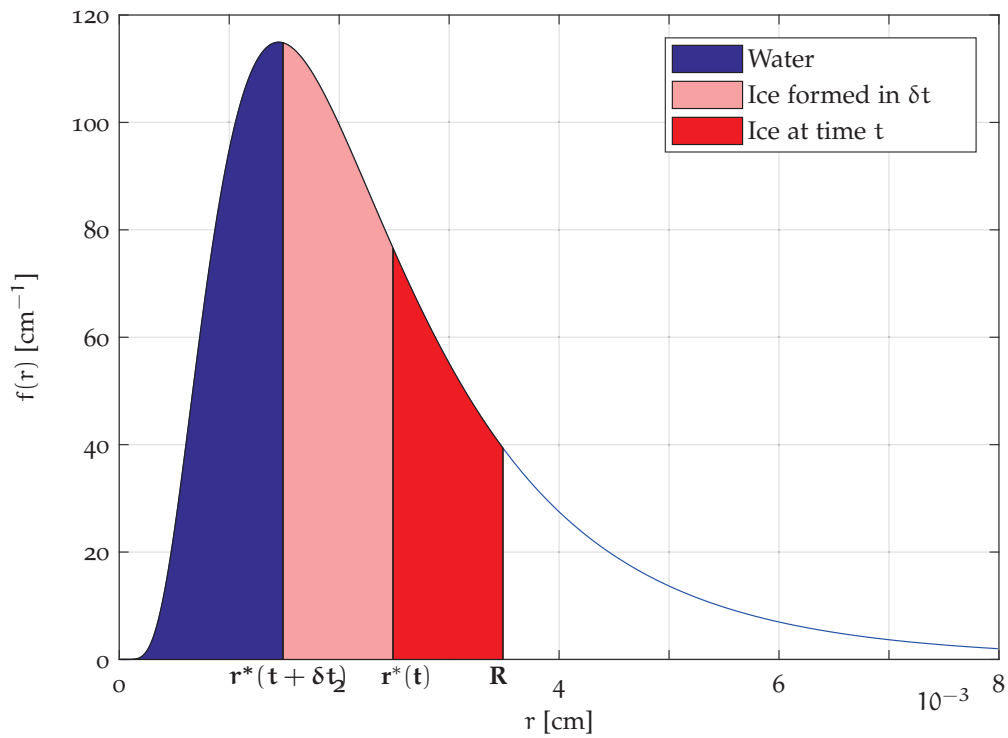

Figure 16: Let us assume that $r^* < R$ and R does not vary in time, i.e. no water is added to the system. Additionally let us assume that $\rho_w = \rho_i$. As temperature falls further consequently $\hat{r}$ becomes smaller and liquid turn into ice.

As before, it is possible to derive the phase transition in terms of ψ. Actually, Eq.(119) may be written as

$$\rho_w \left(\theta_r + \int_{-\infty}^{\Psi} g(\psi) d\psi \right) = \rho_w \left(\theta_r + \int_{-\infty}^{\psi^*} g(\psi) d\psi \right) + \rho_i \int_{\psi^*}^{\Psi} g(\psi) d\psi \quad (124)$$

Deriving with respect to time yields

$$\rho_w \frac{\partial}{\partial t} \int_{-\infty}^{\Psi} g(\psi) d\psi = \rho_w \frac{\partial \psi^*}{\partial t} g(\psi^*) + \rho_i \left(\frac{\partial \Psi}{\partial t} g(\Psi) - \frac{\partial \psi^*}{\partial t} g(\psi^*) \right) \quad (125)$$

According to the definition of ψ^*, Eq.(115), its time derivative becomes

$$\frac{\partial \psi^*}{\partial t} = \begin{cases} \dfrac{\partial \Psi}{\partial t} & \text{if } \hat{r} \geqslant -\dfrac{2\gamma_{aw} \cos \alpha}{\rho_w g \, \Psi} \text{ or } T \geqslant T_m \\[2ex] \dfrac{\partial \hat{\psi}}{\partial t} = \dfrac{l}{g \, T_m} \dfrac{\partial T}{\partial t} & \text{otherwise} \end{cases} \quad (126)$$

Therefore the phase transition may be equivalently expressed as a function of ψ:

$$\frac{\partial \theta_i}{\partial t} = \frac{\partial \Psi}{\partial t} g(\Psi) - \frac{\partial \psi^*}{\partial t} g(\psi^*) \quad (127)$$

COMPARISON WITH DALL'AMICO'S MODEL   Even though this model is based on the same assumptions of Dall'Amico's one, the phase change of water is obtained in a slightly different way.

In this work the variation in time of the ice content is derived extending Kosugi's water retention model [50] to the case of freezing soil using the Gibbs-Thomason equation. Using the Gibbs-Thomson equation it is possible to know the pore radius at which the equilibrium between ice and water takes place, thus the ice content is determined likewise the liquid water content, Eq.(111).

Dall'Amico [17] [16] starting from the Clausius-Clapeyron equation coupled with the *freezing=drying* assumption derived both the formulation for the freezing-point depression due to capillary forces and one for the unfrozen water pressure. Actually, according with the *freezing=drying* assumption, freezing (thawing) water is like evaporating (condensing) water [16] and this means a variation of the liquid water pressure. Using the notation proposed by Dall'Amico [16] the formulation of the liquid water suction $\psi(T)$ under freezing conditions [16], valid both for saturated and unsaturated soils, is

$$\psi(T) = \psi_{w0} + \frac{l}{g \, T^*} (T - T^*) \mathbf{H}(T^* - T) \quad (128)$$

where $\mathbf{H}$ is the Heaviside function, and ψ_{w0} denotes the suction corresponding to the total water content (i.e. ψ_{w0} is analogous to Ψ). Dall'Amico proposed to model the soil water retention curve according with the Van Genuchten model, thus the total water content becomes:

$$\theta = \theta_r + (\theta_s - \theta_r)\{1 + [-\alpha\psi_{w0}]^n\}^{-m} \quad (129)$$

whilst the liquid water content is:

$$\theta_w(T) = \theta_r + (\theta_s - \theta_r)\{1 + [-\alpha\psi(T)]^n\}^{-m} \quad (130)$$

The above equation can be interpreted as an extension of the soil water retention curve which takes in to account of the soil temperature. Usually Eq.(130) is referred to as soil freezing characteristic curve. Therefore one obtains several Soil Freezing Characteristic Curves (SFC): $\theta_w = \theta_w(T)|_{\psi_{w0}}$ that represent the allowed unfrozen water content at a given ψ_0 as a function of temperature [17]. Finally the ice content is determined as

$$\theta_i = \frac{\rho_w}{\rho_i}\{\theta(\psi_{w0}) - \theta_w[\psi(T)]\}, \tag{131}$$

and under the assumption of rigid soil (i.e $\rho_w = \rho_i$) it becomes:

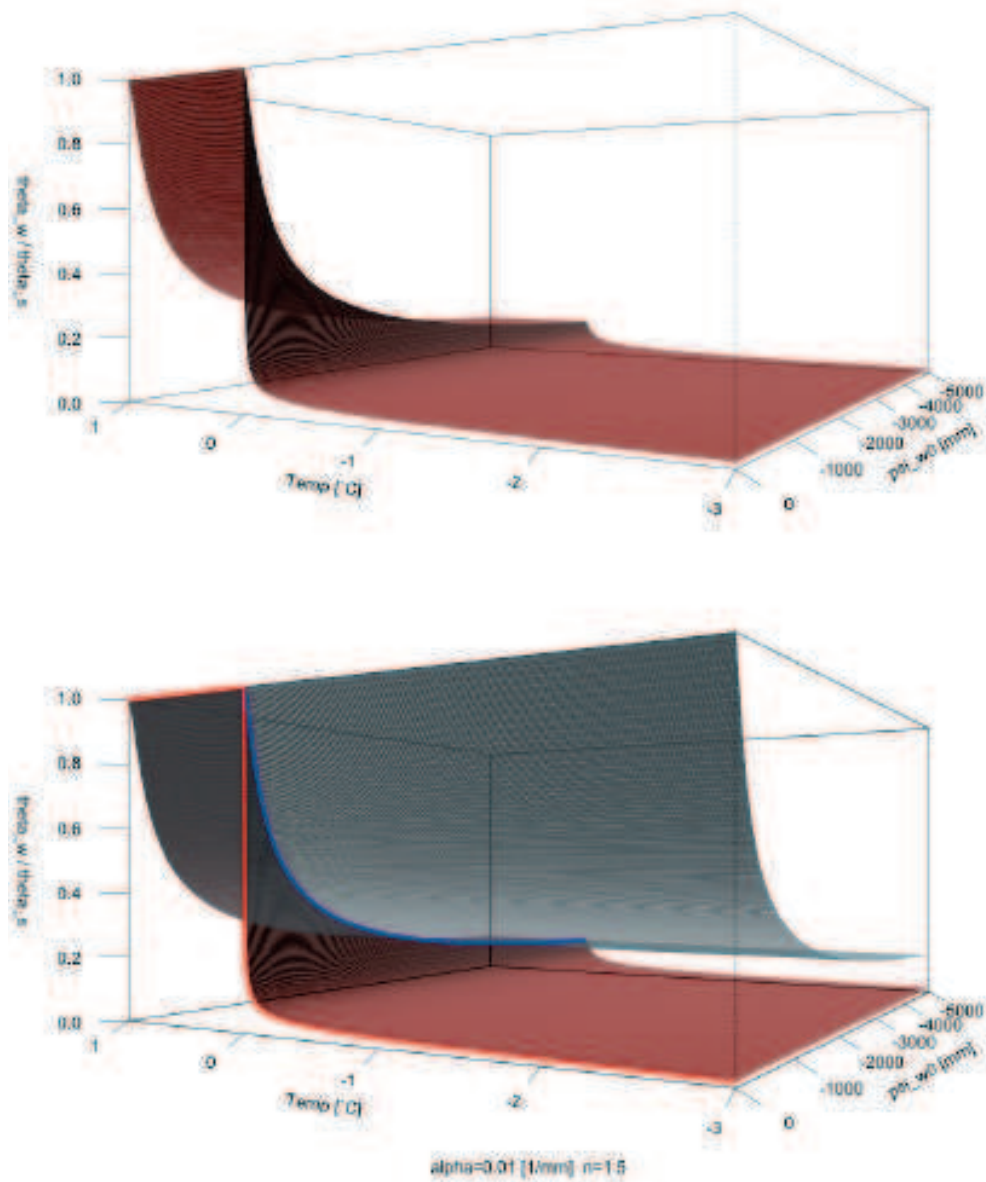$$\theta_i = \theta(\psi_{w0}) - \theta_w[\psi(T)] \tag{132}$$

Figure 17: Top: the red surface represent the ration θ_w/θ_s at different temperatures and various total water content given by ψ_{w0}. Bottom: the blue surface represent the total water content admitted by ψ_{w0}, i.e. the upper boundary of the liquid water. Among the surfaces lies the ice region. Red line: SFC at complete saturation, i.e. when ψ_{w0}. Blue line: SWRC at positive temperatures, [17].

4.5 MASS CONSERVATION EQUATION

Looking at Fig.(10) and by making use of Eq.(120) the mass conservation in a control volume may be described as

$$\rho_w \frac{\partial \theta_w}{\partial t} + \rho_i \frac{\partial \theta_i}{\partial t} = -\rho_w \nabla \cdot \vec{J}_w \qquad (133)$$

According with the *freezing=drying* assumption the flux is allowed only for liquid water, so it just depends on the gradient of liquid water

$$\vec{J}_w = -K(\psi^*)\vec{\nabla}(\psi^* + z) \qquad (134)$$

where, and $K(\psi^*)$ is the hydraulic conductivity that depends on the liquid water saturation degree, and ψ^* is defined as in Eq.(115). The mass conservation , Eq.(133), has to be coupled with two closure equations one relating the water content and suction, the other one for hydraulic conductivity and water content.

The boundary conditions at the ground surface are specified by prescribing precipitation J, and the evapotranspitation, E_T. The boundary condition at the bottom of the domain is specified by prescribing the water flow, $\vec{J}_w$. Using Eq.(125) in Eq.(133) gives

$$\rho_w \frac{\partial \psi^*}{\partial t} g(\psi^*) + \rho_i \left(\frac{\partial \Psi}{\partial t} g(\Psi) - \frac{\partial \psi^*}{\partial t} g(\psi^*) \right) = \rho_w \nabla \cdot [K(\psi^*)\vec{\nabla}(\psi^* + z)] \quad (135)$$

The mass conservation written as in Eq.(135) can be seen as a generalization, taking into account the water phase change, of the well known Richards' equation used to model the flow of water in unsaturated soil. As a matter of fact, according to Eq.(115) and Eq.(126), if we assume that $T \geqslant T_m$, thus there is no ice so the total water content θ coincides with the liquid water content θ_w, then the mass conservation equation, Eq.(135), simplifies as

$$\rho_w \frac{\partial \Psi}{\partial t} g(\Psi) = \rho_w \nabla \cdot [K(\Psi)\vec{\nabla}(\Psi + z)] \qquad (136)$$

It is worthwhile to underline that the left hand side term of the above equation, consistently with Eq.(112), may be written as

$$\rho_w \frac{\partial \Psi}{\partial t} g(\Psi) = \rho_w \frac{\partial \theta}{\partial t} \qquad (137)$$

and substituting in Eq.(136) yields:

$$\rho_w \frac{\partial \theta}{\partial t} = \rho_w \nabla \cdot [K(\Psi)\vec{\nabla}(\Psi + z)] \qquad (138)$$

Since under unsaturated condition it assumed to be a direct correspondence between the pore radius and the capillary pressure, Eq.(138) is properly the Richards' equation.

However the mass conservation as written in Eq.(135) takes into account of the different density of water and ice that will lead to freezing-induced soil deformation. Therefore, beyond the energy conservation equation it will be necessary to provide a soil mechanical model ables to accomplish soil deformation. To overcame this problem, the *freezing=drying* assumption

is used. Therefore, consistently with this hypothesis the water density is set equal to the ice one and Eq.(135) becomes

$$\frac{\partial \theta}{\partial t} := \frac{\partial \Psi}{\partial t} g(\Psi) = \nabla \cdot [K(\psi^*)\vec{\nabla}(\psi^* + z)] \tag{139}$$

The above equation states that the variation of the total water content is due to the flux of liquid water.

Now it possible to express the variation in time of the liquid water content as the difference of the total water content and the ice content:

$$\frac{\partial \theta_w}{\partial t} = \frac{\partial \theta}{\partial t} - \frac{\partial \theta_i}{\partial t} \tag{140}$$

where the the ice variation in time is expressed by Eq.(123)

4.6 THE SOIL ENERGY CONTENT

The energy content $\mathcal{E}$ of the soil volume V_c is

$$\mathcal{E} = U + E_k + E_p \tag{141}$$

where U is the internal energy, E_k the kinetic energy, and E_p the potential energy. Studying the water flow in soils the kinetic energy may be neglected since the water velocities are small.

The internal energy, neglecting the energy of air and excluding the work of volume expansion passing from the liquid to frozen state, consistently with the *freezing=drying* assumption, can be calculated as the sum of the internal energy of the soil particles, ice and liquid water:

$$U = U_s + U_i + U_w \tag{142}$$

hence

$$U = H_s + h_i M_i + h_w M_w \tag{143}$$

where H_s, h_i, h_w are respectively the enthalpy of the soil particles, the specific enthalpy of ice, and the specific enthalpy of water. The specific enthalpy of water can be calculated as

$$\int h_w dT = h_w° + c_w(T - T_{ref}) \tag{144}$$

where h_wř is the specific enthalpy of water at reference temperature T_{ref}, c_w is the specific thermal capacity of water. In the same manner for ice, one obtains

$$\int h_i dT = h_i° + c_i(T - T_{ref}) \tag{145}$$

where h_iř is a the specific enthalpy of ice at reference temperature T_{ref}, c_i is the specific thermal capacity of ice. The difference

$$h_w° - h_i° = l \tag{146}$$

equals the latent heat of fusion. Eventually, posing $T_{ref} = T_m$ and $h_i\check{r} = 0$, the enthalpies of water and ice become:

$$H_w = M_w L + M_w c_w (T - T_m) = \rho_w V_w l + \rho_w V_w c_w (T - T_m) \qquad (147a)$$

$$H_i = M_i c_i (T - T_m) = \rho_i V_i c_i (T - T_m) \qquad (147b)$$

Finally, Eq.(142) can be written as

$$U = \rho_s V_s c_s (T - T_m) + \rho_i V_i c_i (T - T_m) + \rho_w V_w l + \rho_w V_w c_w (T - T_m) \quad (148)$$

Dividing Eq.(148) by the soil volume V_c one obtains the internal energy per unit volume

$$u = u_s + u_i + u_{sp} = \rho_s c_s (T - T_{ref})(1 - \theta_s) + \rho_i c_i (T - T_{ref})\theta_i$$
$$+ \rho_w [l + c_w (T - T_{ref})]\theta_w \quad (149)$$

The potential energy can be calculated as the sum of the potential energy of the ice and liquid water:

$$E_p = E_{p,i} + E_{p,w} \qquad (150)$$

in which the potential energy of the soil is neglected since it is assumed not to vary. Thus the potential energy for a unit volume of soil can be written as

$$E_p = \rho_i V_i gz + \rho_w V_w gz \qquad (151)$$

and dividing by the soil volume V_c one obtains

$$e_p = \rho_i \theta_i gz + \rho_w \theta_w gz \qquad (152)$$

which represent the potential energy per unit volume.

4.7 ENERGY CONSERVATION EQUATION

As seen before the energy conservation can be usefully represented using a Petri's net, Fig.(11). Considering a soil volume one obtains

$$\frac{\partial}{\partial t}(\varepsilon) = \frac{\partial}{\partial t}(u + e_p) = -\nabla \cdot (\vec{J}_w + \vec{J}_g) \qquad (153)$$

where:

- $\vec{J}_g$ is the conduction flux, according to Fourier's law, may be written as

$$\vec{J}_g = -\lambda \vec{\nabla} T \qquad (154)$$

  where λ is the thermal conductivity of the soil that depends on the thermal conductivity of soil particles, and on the proportions of ice and water [17].

- $\vec{J}_w$ is the heat advected by flowing water, and may be written as

$$\vec{J}_w = \rho_w [l + c_w (T - T_m)]\vec{J}_w \qquad (155)$$

The heat advection is due only by liquid water flow according with t

The boundary condition at the ground surface are specified by prescribing the net radiation R_n, and the heat fluxes due to the precipitation, $\underline{J}$, evapotranspiration, $\underline{E}_T$, and the sensible heat $\mathcal{H}$.

The boundary condition at the bottom of the domain are specified by prescribing both the conduction flux, $\vec{\jmath}_g$, and the heat advected by flowing water, $\vec{\jmath}_w$.

Deriving the right hand side of Eq.(153) one obtains

$$\frac{\partial}{\partial t}(u + e_p) = [\rho_s(1 - \theta_s)c_s + \rho_i\theta_i c_i + \rho_w\theta_w c_w]\frac{\partial T}{\partial t}$$
$$+ \rho_w\,[l + c_w(T - T_m) + gz]\frac{\partial\theta_w}{\partial t} + \rho_i[c_i(T - T_m) + gz]\frac{\partial\theta_i}{\partial t} \quad (156)$$

Let us define

$$C_T := \rho_s c_s(1 - \theta_s) + \rho_i\theta_i c_i + \rho_w\theta_w c_w \quad (157)$$

the total thermal capacity of the soil volume. As we can see in Eq.(156), the variation in time of the total energy may be seen as the sum of three contributes: the first term of the right hand side is the sensible part and takes into account of the variation of temperature in time, whilst the last two terms take into account of the variation of the ice and water content.

Substituting Eq.(156) and Eq.(157) into Eq.(153) gives the following equation

$$C_T\frac{\partial T}{\partial t} + \rho_w\,[l + c_w(T - T_m) + gz]\frac{\partial\theta_w}{\partial t} + \rho_i[c_i(T - T_m) + gz]\frac{\partial\theta_i}{\partial t} =$$
$$-\nabla \cdot (\vec{\jmath}_w + \vec{\jmath}_g) \quad (158)$$

Using Eq.(140) in Eq.(158) gives

$$C_T\frac{\partial T}{\partial t} + \rho_w\,[l + c_w(T - T_m) + gz]\left(-\nabla \cdot \vec{\jmath}_w - \frac{\rho_i}{\rho_w}\frac{\partial\theta_i}{\partial t}\right)$$
$$+ \rho_i[c_i(T - T_m) + gz]\frac{\partial\theta_i}{\partial t} = -\nabla \cdot (\vec{\jmath}_w + \vec{\jmath}_g) \quad (159)$$

Finally the energy conservation can be written as

$$C_T\frac{\partial T}{\partial t} - \rho_i l\frac{\partial\theta_i}{\partial t} + \rho_i[(c_w - c_i)(T - T_m)]\frac{\partial\theta_i}{\partial t}$$
$$+ \rho_w c_w\vec{\jmath}_w \cdot \vec{\nabla}T + \rho_w gz\nabla \cdot \vec{\jmath}_w - \nabla \cdot \vec{\jmath}_g = 0 \quad (160)$$

Substituting the time derivative of the ice content, Eq.(110), into the above equation, and since $\rho_w = \rho_i$ yields

$$C_T\frac{\partial T}{\partial t} - \rho_i l\left(\frac{\partial\Psi}{\partial t}g(\Psi) - \frac{\partial\psi^*}{\partial t}g(\psi^*)\right)$$
$$- \rho_i[(c_w - c_i)(T - T_m)]\left(\frac{\partial\Psi}{\partial t}g(\psi) - \frac{\partial\psi^*}{\partial t}g(\psi^*)\right)$$
$$+ \rho_i c_w\vec{\jmath}_w \cdot \vec{\nabla}T + \rho_w gz\nabla \cdot \vec{\jmath}_w - \nabla \cdot \vec{\jmath}_g = 0 \quad (161)$$

The energy conservation equation, Eq.(161), can be analyzed both in presence and absence of ice according with Eq.(115) and Eq.(126).

Let us assume there is no ice, hence we have

$$\psi^* = \Psi, \qquad \frac{\partial \psi^*}{\partial t} = \frac{\partial \Psi}{\partial t} \qquad (162)$$

respectively. Therefore Eq.(161) becomes

$$C_T \frac{\partial T}{\partial t} + \rho_w c_w \vec{J}_w \cdot \vec{\nabla} T + \rho_w g z \nabla \cdot \vec{J}_w - \nabla \cdot \vec{J}_g = 0 \qquad (163)$$

and according with Eq.(115) the water flux is expressed as

$$\vec{J}_w = -K(\Psi) \vec{\nabla} (\Psi + z)] \qquad (164)$$

Otherwise, when ice occurs, Eq.(115) and Eq.(126) yields

$$\psi^* = \hat{\psi}, \qquad \frac{\partial \psi^*}{\partial t} = \frac{l}{g\, T_m} \frac{\partial T}{\partial t} \qquad (165)$$

respectively. Therefore Eq.(161) becomes

$$
\begin{aligned}
C_T \frac{\partial T}{\partial t} - \rho_i l &\left(\frac{\partial \Psi}{\partial t} g(\Psi) - \frac{l}{g\, T_m} \frac{\partial T}{\partial t} g(\hat{\psi}) \right) \\
&- \rho_i [(c_w - c_i)(T - T_m)] \left(\frac{\partial \Psi}{\partial t} g(\Psi) - \frac{l}{g\, T_m} \frac{\partial T}{\partial t} g(\hat{\psi}) \right) \\
&+ \rho_i c_w \vec{J}_w \cdot \vec{\nabla} T + \rho_w g z \nabla \cdot \vec{J}_w - \nabla \cdot \vec{J}_g = 0 \quad (166)
\end{aligned}
$$

where the water flux is expressed as

$$\vec{J}_w = \nabla \cdot [K(\hat{\psi}) \vec{\nabla} (\hat{\psi} + z)] \qquad (167)$$

Eq.(166) can be rewrite as

$$
\begin{aligned}
C_T \frac{\partial T}{\partial t} + \rho_i \left[l + (c_w - c_i)(T - T_m) \right] \frac{l}{g\, T_m} \frac{\partial T}{\partial t} g(\hat{\psi}) \\
- \rho_i \left[l + (c_w - c_i)(T - T_m) \right] \frac{\partial \Psi}{\partial t} g(\Psi) \\
+ \rho_i c_w \vec{J}_w \cdot \vec{\nabla} T + \rho_w g z \nabla \cdot \vec{J}_w - \nabla \cdot \vec{J}_g = 0 \quad (168)
\end{aligned}
$$

where the term:

$$C_T + \rho_i \left[l + (c_w - c_i)(T - T_m) \right] \frac{l}{g\, T_m} g(\hat{\psi}) = C_T + C_{ph} := C_a \qquad (169)$$

is usually referred to as the apparent heat capacity and is the sum of two contributes: C_T which accounts for the sensible heat transmitted to the soil matrix, and C_{ph} which account for the latent heat released by phase change. Finally the equation for the energy conservation may be written as:

$$
\begin{aligned}
C_{ph} \frac{\partial T}{\partial t} - \rho_i \left[l + (c_w - c_i)(T - T_m) \right] \frac{\partial \Psi}{\partial t} g(\Psi) \\
+ \rho_i c_w \vec{J}_w \cdot \vec{\nabla} T + \rho_w g z \nabla \cdot \vec{J}_w - \nabla \cdot \vec{J}_g = 0 \quad (170)
\end{aligned}
$$

5 | CONCLUSIONS

In this work the equations for the water flow in an unsaturated freezing soil and the coupled energy conservation have been derived. This was achieved starting from the basic principles of thermodynamics and the theory of the water flow in unsaturated unfrozen soils according with Mualem's assumption [72]).

Starting from the fact that water in soils freezes over a range of temperature determined by the capillary forces and dissolved solutes, the derivation of the mass conservation equation has firstly required to determine the freezing depression point of soil water. Thus, according with the *freezing=drying* and the thermodynamic equilibrium assumptions (see Sec.(4.1)) the Gibbs-Thomson equation Eq.(98) was throughly derived considering a capillary tube within which a water solution is in equilibrium with ice [17] [2]. From this equation it is possible to determine for each temperature below T_m the capillary radius at which the thermodynamic equilibrium between liquid water and ice is reached.

Since a volume of soil may be presented as an equivalent bundle of capillaries, with identical retention properties as the real soil [51], this result has been straightforward applied to Kosugi's two-parameters retention model in order to determine at every temperature and how much water is liquid and how much is ice (see Sec.(4.4.2)). Doing this a restriction on the radius of the ice-water interface has been introduced to guarantee that it is not possible to freeze/thaw more water than that is present in the soil. Additionally, this approach allowed to derive an explicit equation for the variation in time of the ice content (see Sec.(4.4.3)). Thanks the Young-Laplace under unsaturated condition it is possible to express the water content, the ice content, and the phase transition equation without regard as a function either of the pore radius or of the pressure. Hence the equation for the total water content conservation has been obtained imposing $\rho_w = \rho_i$ according with the rigid soil scheme, and modeling the water flux with Darcy's Buckingham's equation. The water flux within a frozen soil is assumed analogous to that in unsaturated soil, according to the *freezing=drying* assumption [68]. Finally the liquid water is obtained as the difference between the the total water content and the ice content.

Regarding the energy conservation equation, within the local averaging volume, it was derived assuming that soil particles, ice and liquid water are at the thermodynamic equilibrium, i.e. all of them have the same temperature, the air phase is neglected as well the kinetic energy of water since velocities in porous media are small, and the potential energy of soil since it is assume that it does not change. Additionally the *freezing=drying* assumption and the rigid soil scheme, i.e. $p_i = p_a \leftarrow 0$ and $\rho_w = \rho_i$ respectively, allowed to neglect the work due freezing expansion.

The result is a system of two coupled non linear differential equations on the unknowns (ψ, T). Thus thanks to the mass conservation equation the water flow and the phase change is modeled. Including the water flow it is possible to model the heat advection in the energy conservation that as discussed in the first chapter has a significant importance. Furthermore a physical-based equation for the phase change allows the treatment of the latent heat in the heat equation as an apparent heat capacity. In addition to the soil water retention curve and relative hydraulic conductivity it is necessary to provide two further closure equations one for the thermal conductivity and one for the capacity both dependent on the ice and water content [17]. So far a numerical scheme to solve this system is not provided. It was shown (3.3) that when ice does not occur the mass and energy conservation equation for freezing soils naturally modify to those derived for the unfrozen soils. In the latter case the equations for the mass conservation may be conveniently solved with the nested Newton algorithm proposed by Casulli and Zanolli [14]. Although Casulli and Zanolli presented the nested Newton by making use of Brooks and Corey soil water retention model and Van Genuchten one, it is worthwhile to underline that Kosugi's two-parameter retention model satisfies the mathematical requirement to apply this numerical scheme as well as Brook and Corey, and Van Genuchten ones. With regards the energy conservation equation it may be efficiently solve with an implicit up-wind finite different scheme [29]. Additionally this model will have to be included into an hydrological model in order to provide the right definition of boundaries conditions.

The main feature of this model is represented by making use of the Kosugi's model to derive the soil hydraulic properties starting from the knowledge of the pore-size distribution. This model coupled with the Gibbs-Thomson equation, derived as a function of the pore radius and osmotic pressure of the solution, has been extended to the case of freezing soils.

A number of unresolved theoretical issues persist for simulating coupled thermal and hydraulic processes in freezing or thawing soils:

- coupling Kosugi's water retention model and the Gibbs-Thomson equation allowed to derive the equations for the mass and energy conservation for unsaturated freezing soils. This model should be properly extended in order to deal with the freezing/thawing processes under saturated condition. Actually, under saturated condition the water pressure is just determined by the water table level. So water is not subjected anymore to the capillary forces and it is not possible to determine a one-to-one relationship between water pressure and pore radius. Furthermore the freezing temperature varies with temperature according with Clausius-Clapeyron equation [16]. Whilst in presence of capillary forces water freezes at temperature below T_m, and the liquid water content and the ice content may be determined using the Gibbs-Thomson equation, under saturated conditions water may freezes at temperature above T_m but the model as presented so far does not allows to determine how much water turns into ice and vice versa. On the contrary, Dall'Amico proposed a model in which the phase change is derived by the Clausius-Clapeyron equation and

hence this model may take into account of freezing variably-saturated soil.

- the *freezing-drying* assumption does not allow to properly model the ice pressure. Of course this issue depends on the model scope, becomes important dealing with freezing-induced mechanical deformations. In the latter case it will be necessary to provide the definition of a soil mechanic model.

- As pointed out by Kurylyk [54] the freezing/thawing processes do not occur at the thermodynamic equilibrium since the ice formation is characterized by a nucleation processes during which the latent heat is exchanged. This is an issue explored in some paper experimentally [105] but which still did not have, at our knowledge, a convincing theoretical assessment.

A | PETRI NETS

Petri Nets are graphical and mathematical modeling tool that allow to provide a graphical representation of the interactions that a system is subject to [73]. Petri Nets were developed to study discrete and time independent systems. The system is shown as a directed, wighted, bipartite graph consisting of two kinds of nodes, called places and transition, where arcs are either from a place to a transition or from a transition to a place [73].

However, it is possible to modify Petri nets including the time dependence with the view to study dynamical system such as hydrological ones. In this case we talk about time continuous Petri nets, TCPN.

The graphical representation of a system foresees that:

- places, now called *storages* are drawn as circles. The storage is identified by a variable specification and eventually by a color to represent the same physical place but in different types of budgets. From a mathematical viewpoint a storage represents the time variation of the named quantity.

- transitions, called *fluxes* are represented as bars or boxes. As for storages, fluxed are denoted by a variable specification. A table of association enables to connect each flux with its own mathematical expression that can be either algebraic or differential.

- arcs connect a places with a transition and vice versa. By convention, the arc is drawn with the same color of the place from where it exists and is positive in the direction of the arrow. By the definition of a bipartite graph the only allowed connection are among a storage and one or more fluxes or vice versa, Fig.(18).

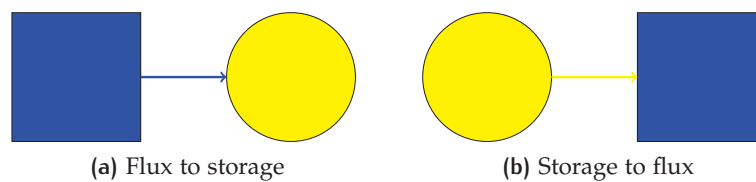(a) Flux to storage   (b) Storage to flux

Figure 18: Allowed connections in Petri Nets

The connection *one to more* foreseen the definition of a partition coefficient. It is set the possibility that a storage is double connected with a flux. This simply means that there is a flux from the storage to a metastable state and form this a flux towards the storage again as shown in Fig.(19). Different kinds of arcs are defined each one to represent

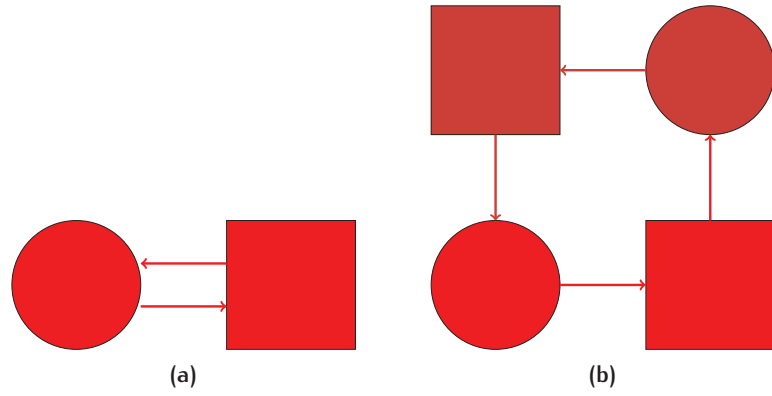A time continuous Petri net can be uniquely identified by:

Figure 19: The double connection shown in (a) is explicated in (b) where the dark color represents the metastable state.

- $P = \{p_1, \ldots, p_j, \ldots, p_n\}$ is the set of places.

- $T = \{t_1, \ldots, t_i, \ldots, t_l\}$ is the set of transitions.

- P and T are disjoint, i.e. no object can be both a place and a transition.

- S is the set of tokens present in places at any specific time.

- A is a table in which is explained the semantic of fluxes and symbols.

- E is the set of fluxes expression.

- Pre is the set of arcs between a place to a certain transition. Pre can be defined as a matrix $n \times l$ whose elements are:

$$Pre[j, i] : (P, T) \rightarrow E$$

From this definition it possible to define the preset of each transition t_i as:

$$t_i = p_j | Pre[j, i] > 0$$

- Post is the set of arcs between a transition to a certain place. Post can be defined as a matrix $l \times n$ whose elements are:

$$Post[j, i] : (T, P) \rightarrow E$$

From this definition it is possible to define the postset of each transition t_i as:

$$t_i = p_j | Post[j, i] > 0$$

- $Adj = Pre - Post$ is the adjacency matrix associated to the graph.

Hence time continuous Petri net is defined as a 7-tuple:

$$TCPN = (P, T, Pre, Post, S, A, E) \tag{171}$$

In the light of this, from a TCPN it is possible to write a coupled set of ordinary differential equations, in number equal to the rank of the places:

$$\frac{dp_j}{dt} = \sum_i Post[i, j] - Pre[j, i] \quad \text{for} \quad j = 1, \ldots, n \tag{172}$$

BIBLIOGRAPHY

[1] "Climate change impacts on permafrost engineering design." *Panel on Energy Research and Development, Environment Canada, Ottawa ON, Canada. 42p.*, 1998.

[2] J. P. Acker, J. A. Elliott, and L. E. McGann, "Intercellular ice propagation: experimental evidence for ice growth through membrane pores," *Biophysical journal*, vol. 81, no. 3, pp. 1389–1397, 2001.

[3] I. Allison, R. G. Barry, and B. E. Goodison, *Climate and cryosphere (CliC) project science and co-ordination plan: version 1.* Joint Planning Staff for WCRP, World Meteorological Organization, 2001, vol. 114.

[4] O. Anisimov, N. Shiklomanov, and F. Nelson, "Variability of seasonal thaw depth in permafrost regions: a stochastic modeling approach," *Ecological Modelling*, vol. 153, no. 3, pp. 217–227, 2002.

[5] L. U. Arenson, S. M. Springman, Sego, and C. Dave, "The rheology of frozen soils," *Applied Rheology*, vol. 17, no. 1, p. 12147, 2007.

[6] R. G. Barry, "The parameterization of surface albedo for sea ice and its snow cover," *Progress in Physical Geography*, vol. 20, no. 1, pp. 63–79, 1996.

[7] J. Brown, O. J. F. Jr, J. A. Heginbottom, and E. S. Melnikov, "Circum-Arctic map of permafrost and ground-ice conditions," no. 45, 1997.

[8] J. Brown, S. L. Smith, V. Romanovsky, H. H. Christiansen, G. Clow, and F. E. Nelson, "Global terrestrial network for permafrost [GTN-P]," *Terrestrial Essential Climate Variables for Assessment, Mitigation and Adaptation*, pp. 24–25, 2008.

[9] W. Brutsaert, "Probability laws for pore-size distributions," *Soil Science*, vol. 101, no. 2, pp. 85–92, 1966.

[10] N. Burdine *et al.*, "Relative permeability calculations from pore size distribution data," *Journal of Petroleum Technology*, vol. 5, no. 03, pp. 71–78, 1953.

[11] C. Burn, "Permafrost," *Encyclopedia of Quaternary Science*, no. 3, pp. 2191–2199, 2006.

[12] C. Burn and F. Nelson, "Comment on "A projection of severe near-surface permafrost degradation during the 21st century" by David M. Lawrence and Andrew G. Slater," *Geophysical Research Letters*, vol. 33, no. 21, 2006.

[13] S. K. Carey and M.-K. Woo, "Hydrology of two slopes in subarctic Yukon, Canada," *Hydrological Processes*, vol. 13, no. 16, pp. 2549–2562, 1999.

[14] V. Casulli and P. Zanolli, "A nested Newton-type algorithm for finite volume methods solving Richards' equation in mixed form," *SIAM Journal on Scientific Computing*, vol. 32, no. 4, pp. 2255–2273, 2010.

[15] J. Constantz and F. Murphy, "The temperature dependence of ponded infiltration under isothermal conditions," *Journal of hydrology*, vol. 122, no. 1-4, pp. 119–128, 1991.

[16] M. Dall'Amico, S. Endrizzi, S. Gruber, and R. Rigon, "A robust and energy-conserving model of freezing variably-saturated soil," *The Cryosphere*, vol. 5, no. 2, p. 469, 2011.

[17] M. Dall'Amico, "Coupled water and heat transfer in permafrost modeling," Ph.D. dissertation, University of Trento, 2010.

[18] T. N. Davis, *Permafrost: a guide to frozen ground in transition*. University of Alaska Press, 2001.

[19] W. Dobinski, "Permafrost," *Earth-Science Reviews*, vol. 108, no. 3, pp. 158–169, 2011.

[20] W. Durner, "Hydraulic conductivity estimation for soils with heterogeneous pore structure," *Water Resources Research*, vol. 30, no. 2, pp. 211–223, 1994.

[21] O. T. Farouki, *Thermal properties of soils*. Trans Tech Pub., Rockport, MA, 1986.

[22] M. Fauve, H. Rhyner, and M. Schneebeli, "Pistenpräparation und Pistenpflege: ein Handbuch für den Praktiker," 2002.

[23] H. M. French, *The periglacial environment*. John Wiley & Sons, 2013.

[24] M. Fuchs, G. Campbell, and R. Papendick, "An analysis of sensible and latent heat flow in a partially frozen unsaturated soil," *Soil Science Society of America Journal*, vol. 42, no. 3, pp. 379–385, 1978.

[25] H. H. Gerke and M. V. Genuchten, "A dual-porosity model for simulating the preferential movement of water and solutes in structured porous media," *Water resources research*, vol. 29, no. 2, pp. 305–319, 1993.

[26] L. W. Gold and A. H. Lachenbruch, "Thermal conditions in permafrost–A review of North American literature," 1973.

[27] L. W. Gold and G. P. Williams, "An unusual ice formation on the Ottawa River," *Journal of Glaciology*, vol. 4, no. 35, pp. 569–573, 1963.

[28] I. Gouttevin, G. Krinner, P. Ciais, J. Polcher, and C. Legout, "Multi-scale validation of a new soil freezing scheme for a land-surface model with physically-based hydrology," *The Cryosphere*, vol. 6, pp. 407–430, 2012.

[29] D. Greenspan and V. Casulli, *Numerical Analysis for Applied Mathematics, Science, and Engineering*. Boston, MA, USA: Addison-Wesley Longman Publishing Co., Inc., 1988.

[30] S. Gruber, M. Hoelzle, and W. Haeberli, "Rock-wall temperatures in the Alps: modelling their topographic distribution and regional differences," *Permafrost and Periglacial Processes*, vol. 15, no. 3, pp. 299–307, 2004.

[31] K. Hansson, J. Simuunek, M. Mizoguchi, L.-C. Lundin, and M. T. V. Genuchten, "Water flow and heat transport in frozen soil," *Vadose Zone Journal*, vol. 3, no. 2, pp. 693–704, 2004.

[32] J. W. Harden, C. D. Koven, C.-L. Ping, G. Hugelius, A. David McGuire, P. Camill, T. Jorgenson, P. Kuhry, G. J. Michaelson, J. A. O'Donnell, *et al.*, "Field information links permafrost carbon to physical vulnerabilities of thawing," *Geophysical Research Letters*, vol. 39, no. 15, 2012.

[33] R. Harlan, "Analysis of coupled heat-fluid transport in partially frozen soil," *Water Resources Research*, vol. 9, no. 5, pp. 1314–1323, 1973.

[34] C. Harris, L. U. Arenson, H. H. Christiansen, B. Etzelmüller, R. Frauenfelder, S. Gruber, W. Haeberli, C. Hauck, M. Hoelzle, O. Humlum, *et al.*, "Permafrost and climate in europe: Monitoring and modelling thermal, geomorphological and geotechnical responses," *Earth-Science Reviews*, vol. 92, no. 3, pp. 117–171, 2009.

[35] K. M. Hinkel, "Estimating seasonal values of thermal diffusivity in thawed and frozen soils using temperature time series," *Cold Regions Science and Technology*, vol. 26, no. 1, pp. 1–15, 1997.

[36] K. M. Hinkel and S. I. Outcalt, "Detection of nonconductive heat transport in soils using spectral analysis," *Water Resources Research*, vol. 29, no. 4, pp. 1017–1023, 1993.

[37] ——, "Identification of heat-transfer processes during soil cooling, freezing, and thaw in central Alaska," *Permafrost and Periglacial Processes*, vol. 5, no. 4, pp. 217–235, 1994.

[38] A. Instanes, O. Anisimov, L. Brigham, D. Goering, L. N. Khrustalev, B. Ladanyi, and J. O. Larsen, "Chapter 16: Infrastructure: buildings, support systems, and industrial facilities," *Arctic Climate Impact Assessment.[np].*, 2005.

[39] A. Ireson, G. Van Der Kamp, G. Ferguson, U. Nachshon, and H. Wheater, "Hydrogeological processes in seasonally frozen northern latitudes: understanding, gaps and challenges," *Hydrogeology Journal*, vol. 21, no. 1, pp. 53–66, 2013.

[40] K. Jackson and B. Chalmers, "Freezing of liquids in porous media with special reference to frost heave in soils," *Journal of Applied Physics*, vol. 29, no. 8, pp. 1178–1181, 1958.

[41] Y.-W. Jame and D. I. Norum, "Heat and mass transfer in a freezing unsaturated porous medium," *Water Resources Research*, vol. 16, no. 4, pp. 811–819, 1980.

[42] Y. Jiang, Q. Zhuang, S. Schaphoff, S. Sitch, A. Sokolov, D. Kicklighter, and J. Melillo, "Uncertainty analysis of vegetation distribution in the northern high latitudes during the 21st century with a dynamic vegetation model," *Ecology and evolution*, vol. 2, no. 3, pp. 593–614, 2012.

[43] A. Kääb, J. M. Reynolds, and W. Haeberli, "Glacier and permafrost hazards in high mountains," pp. 225–234, 2005.

[44] A. Kade, V. Romanovsky, and D. Walker, "The n-factor of nonsorted circles along a climate gradient in Arctic Alaska," *Permafrost and Periglacial Processes*, vol. 17, no. 4, pp. 279–289, 2006.

[45] B. Kay, M. Fukuda, H. Izuta, and M. I. Sheppard, "The importance of water migration in the measurement of the thermal conductivity of unsaturated frozen soils," *Cold Regions Science and Technology*, vol. 5, no. 2, pp. 95–106, 1981.

[46] F. Keller and H. Gubler, "Interaction between snow cover and high mountain permafrost, Murtel-Corvatsch, Swiss Alps," vol. 1, pp. 332–337, 1993.

[47] F. Keller, W. Haeberli, D. Rickenmann, and H. Rigendinger, "Dämme gegen Naturgefahren: Bau von Schutzdämmen gegen Rüfen und Lawinen in Pontresina," *Tec*, vol. 21, no. 17, pp. 13–17, 2002.

[48] J. Kestin, M. Sokolov, and W. A. Wakeham, "Viscosity of liquid water in the range $-8°C$ to $150°C$," *Journal of Physical and Chemical Reference Data*, vol. 7, no. 3, pp. 941–948, 1978.

[49] L. N. Khrustalev, "Problems of permafrost engineering as related to global climate warming," pp. 407–423, 2001.

[50] K. Kosugi, "Lognormal distribution model for unsaturated soil hydraulic properties," *Water Resources Research*, vol. 32, no. 9, pp. 2697–2703, 1996.

[51] K. Kosugi, J. W. Hopmans, and J. H. Dane, "Methods of soil analysis. part 4. physical methods," 2002.

[52] K. Kosugi, "Three-parameter lognormal distribution model for soil water retention," *Water Resources Research*, vol. 30, no. 4, pp. 891–901, 1994.

[53] B. L. Kurylyk, K. T. B. MacQuarrie, and J. M. McKenzie, "Climate change impacts on groundwater and soil temperatures in cold and temperate regions: Implications, mathematical theory, and emerging simulation tools," *Earth-Science Reviews*, vol. 138, pp. 313–334, 2014.

[54] B. L. Kurylyk and K. Watanabe, "The mathematical representation of freezing and thawing processes in variably-saturated, non-deformable soils," *Advances in Water Resources*, vol. 60, pp. 160–177, 2013.

[55] A. H. Lachenbruch, J. Sass, B. Marshall, and T. Moses, "Permafrost, heat flow, and the geothermal regime at Prudhoe Bay, Alaska," *Journal of Geophysical Research: Solid Earth*, vol. 87, no. B11, pp. 9301–9316, 1982.

[56] M. Larsbo, J. Koestel, and N. Jarvis, "Relations between macropore network characteristics and the degree of preferential solute transport," *Hydrology and Earth System Sciences*, vol. 18, no. 12, p. 5255, 2014.

[57] D. M. Lawrence and A. G. Slater, "A projection of severe near-surface permafrost degradation during the 21st century," *Geophysical Research Letters*, vol. 32, no. 24, 2005.

[58] J. Lindsay and W. Odynsky, "Permafrost in organic soils of northern Alberta," *Canadian Journal of Soil Science*, vol. 45, no. 3, pp. 265–269, 1965.

[59] F. Ling and T. Zhang, "Numerical simulation of permafrost thermal regime and talik development under shallow thaw lakes on the Alaskan Arctic Coastal Plain," *Journal of Geophysical Research: Atmospheres*, vol. 108, no. D16, 2003.

[60] J. G. Lockwood, *Causes of climate*.   Wiley, 1979.

[61] V. J. Lunardini, *Heat transfer in cold climates*.   Van Nostrand Reinhold Company, 1981.

[62] L. Luo, A. Robock, K. Y. Vinnikov, C. A. Schlosser, A. G. Slater, A. Boone, P. Etchevers, F. Habets, J. Noilhan, H. Braden, *et al.*, "Effects of frozen soil on soil temperature, spring infiltration, and runoff: Results from the PILPS 2 (d) experiment at Valdai, Russia," *Journal of Hydrometeorology*, vol. 4, no. 2, pp. 334–351, 2003.

[63] J. Luthin and G. Guymon, "Soil moisture-vegetation-temperature relationships in central Alaska," *Journal of Hydrology*, vol. 23, no. 3-4, pp. 233–246, 1974.

[64] S. Marshall, *The cryosphere*.   Princeton University Press, 2012.

[65] J. M. McKenzie and C. I. Voss, "Permafrost thaw in a nested groundwater-flow system," *Hydrogeology Journal*, vol. 21, no. 1, pp. 299–316, 2013.

[66] J. M. McKenzie, C. I. Voss, and D. I. Siegel, "Groundwater flow with energy transport and water–ice phase change: numerical simulations, benchmarks, and application to freezing in peat bogs," *Advances in water resources*, vol. 30, no. 4, pp. 966–983, 2007.

[67] F. A. Michel and R. O. Van Everdingen, "Changes in hydrogeologic regimes in permafrost regions due to climatic change," *Permafrost and Periglacial Processes*, vol. 5, no. 3, pp. 191–195, 1994.

[68] R. D. Miller, "Phase equilibria and soil freezing," vol. 287, pp. 193–197, 1965.

[69] ——, *Soil freezing in relation to pore water pressure and temperature. 1*, 1973.

[70] ——, "Freezing phenomena in soils," *Applications of soil physics*, vol. 278, p. 283, 1980.

[71] P. Milly, "Estimation of brooks-corey parameters from water retention data," *Water Resources Research*, vol. 23, no. 6, pp. 1085–1089, 1987.

[72] Y. Mualem, "A new model for predicting the hydraulic conductivity of unsaturated porous media," *Water resources research*, vol. 12, no. 3, pp. 513–522, 1976.

[73] T. Murata, "Petri nets: Properties, analysis and applications," *Proceedings of the IEEE*, vol. 77, no. 4, pp. 541–580, 1989.

[74] F. H. Nicholson, "Permafrost modification by changing the natural energy budget," pp. 62–67, 1978.

[75] J. Nimmo, "Porosity and pore size distribution," *Encyclopedia of Soils in the Environment*, vol. 3, pp. 295–303, 2004.

[76] J. F. Nixon and B. Ladany, *Thaw consolidation. In Geotechnical engineering for cold regions*. McGraw-Hill, 1978.

[77] H. Othmer, B. DiekkrÜger, and M. Kutilek, "Bimodal porosity and unsaturated hydraulic conductivity." *Soil Science*, vol. 152, no. 3, pp. 139–150, 1991.

[78] S. I. Outcalt, F. E. Nelson, and K. M. Hinkel, "The zero-curtain effect: Heat and mass transfer across an isothermal region in freezing soil," *Water Resources Research*, vol. 26, no. 7, pp. 1509–1516, 1990.

[79] P. P. Overduin, D. L. Kane, and W. K. van Loon, "Measuring thermal conductivity in freezing and thawing soil using the soil temperature response to heating," *Cold Regions Science and Technology*, vol. 45, no. 1, pp. 8–22, 2006.

[80] A. Phukan, *Frozen Ground Engineering*, 1985.

[81] W. Quinton, T. Shirazi, S. Carey, and J. Pomeroy, "Soil water storage and active-layer development in a sub-alpine tundra hillslope, southern Yukon Territory, Canada," *Permafrost and Periglacial Processes*, vol. 16, no. 4, pp. 369–382, 2005.

[82] B. R. and C. A. T., "Hydraulic properties of porous media," *Colorado State University, Hydro Paper*, vol. 3, p. 27, 1964.

[83] L. A. Richards, "Capillary conduction of liquids through porous mediums," *Physics*, vol. 1, no. 5, pp. 318–333, 1931.

[84] D. W. Riseborough, *Modeling climatic influences on permafrost at boreal forest site.*, 1985.

[85] D. Riseborough, N. Shiklomanov, B. Etzelmüller, S. Gruber, and S. Marchenko, "Recent advances in permafrost modelling," *Permafrost and Periglacial Processes*, vol. 19, no. 2, pp. 137–156, 2008.

[86] V. E. Romanovsky and T. E. Osterkamp, "Inter annual variation of the thermal regime of the active layer and near-surface permafrost in northern Alaska," *Permafrost and Periglacial Processes*, no. 6, p. 313, 1995.

[87] ——, "Thawing of the active layer on the coastal plain of the Alaskan Arctic," *Permafrost and Periglacial Processes*, vol. 8, no. 1, pp. 1–22, 1997.

[88] P. J. Ross and K. R. Smettem, "Describing soil hydraulic properties with sums of simple functions," *Soil Science Society of America Journal*, vol. 57, no. 1, pp. 26–29, 1993.

[89] W. R. Rouse, "Microclimate of Arctic tree line. 2: Soil microclimate of tundra and forest." *Water resources Research*, vol. 20, no. 1, pp. 67–73, 1984.

[90] S. Safran, *Statistical thermodynamics of surface, interfaces, and membranes*. Reading, Massachusetts: Addison-Wesley, 1994.

[91] P. Schoeneich, M. Dall'Amico, P. Deline, and A. Zischg, "Hazards related to permafrost and to permafrost degradation." *PermaNET project, state-of-the-art report 6.2.*, 2011.

[92] M. C. Serreze, R. C. Schnell, and J. D. Kahl, "Low-level temperature inversions of the eurasian arctic and comparisons with soviet drifting station data," *Journal of Climate*, vol. 5, no. 6, pp. 615–629, 1992.

[93] T. G. Smirnova, J. M. Brown, S. G. Benjamin, and D. Kim, "Parameterization of cold-season processes in the maps land-surface scheme," *Journal of Geophysical Research: Atmospheres*, vol. 105, no. D3, pp. 4077–4086, 2000.

[94] M. Smith, "The significance of climate change for the permafrost environment," *Climate change impacts in the Canadian artic*, pp. 67–81, 1986.

[95] E. J. Spaans and J. M. Baker, "The soil freezing characteristic: Its measurement and similarity to the soil moisture characteristic," *Soil Science Society of America Journal*, vol. 60, no. 1, pp. 13–19, 1996.

[96] S. M. Springman and L. U. Arenson, "Recent advances in permafrost geotechnics," in *Proceedings of the 9th International Conference on Permafrost*, vol. 29, 2008, pp. 1685–1694.

[97] M. B. Stevens, J. E. Smerdon, J. F. González-Rouco, M. Stieglitz, and H. Beltrami, "Effects of bottom boundary placement on subsurface heat storage: Implications for climate model simulations," *Geophysical research letters*, vol. 34, no. 2, 2007.

[98] T. Thiis and C. Jaedicke, "Changes in the snowdrift pattern caused by a building extension–investigations through scale modelling and numerical simulations," in *Snow Engineering: Recent Advances and Developments. Proceedings of the Fourth International Conference on Snow Engineering.*, 2000.

[99] H. R. Thomas, P. J. Cleall, Y. Li, C. Harris, and M. Kern-Luetschg, "Modelling of cryogenic processes in permafrost and seasonally frozen soils," *Geotechnique*, vol. 59, no. 3, pp. 173–184, 2009.

[100] G. Van der Kamp, M. Hayashi, and D. Gallen, "Comparing the hydrology of grassed and cultivated catchments in the semi-arid Canadian prairies," *Hydrological Processes*, vol. 17, no. 3, pp. 559–575, 2003.

[101] R. O. Van Everdingen, *Multi-Language Glossary of Permafrost and Related Ground-Ice Terms in Chinese, English, French, German, Icelandic, Italian, Norwegian, Polish, Romanian, Russian, Spanish, and Swedish.* International Permafrost Association, Terminology Working Group, 1998.

[102] M. T. Van Genuchten, "A closed-form equation for predicting the hydraulic conductivity of unsaturated soils," *Soil science society of America journal*, vol. 44, no. 5, pp. 892–898, 1980.

[103] P. Viterbo, A. Beljaars, J.-F. Mahfouf, and J. Teixeira, "The representation of soil moisture freezing and its impact on the stable boundary layer," *Quarterly Journal of the Royal Meteorological Society*, vol. 125, no. 559, pp. 2401–2426, 1999.

[104] J. Wallace and P. Hobbs, "Atmosphere science-an introductory survey." *Atmospheric Science*, vol. 1, 1977.

[105] X. Wan and Y. Lai, "Experimental study on water freezing process in chloride saline soils," *Journal of Physical and Chemical Reference Data*, vol. 7, no. 3, pp. 941–948, 1978.

[106] M. Wegmann, "Frostdynamik in hochalpinen Felswänden am Beispiel der Region Jungfraujoch- Aletsch," *Mitteilungen der Versuchsanstalt fur Wasserbau, Hydrologie und Glaziologie an der Eidgenossischen Technischen Hochschule Zurich*, 1998.

[107] J. R. Williams, *Ground water in the permafrost regions of Alaska.* US Government Printing Office, 1970, vol. 696.

[108] P. Williams and M. Smith, *The frozen earth: fundamentals of geocryology.* Cambridge [etc.]: Cambridge University Press, 1989.

[109] J. Wolfe and G. Bryant, "Cellular cryobiology: thermodynamic and mechanical effects," *International Journal of Refrigeration*, vol. 24, no. 5, pp. 438–450, 2001.

[110] E. D. Yershov and P. J. Williams, *General geocryology.* Cambridge university press, 2004.

[111] S. Yi, M. A. Arain, and M.-K. Woo, "Modifications of a land surface scheme for improved simulation of ground freeze-thaw in northern environments," *Geophysical Research Letters*, vol. 33, no. 13, 2006.

[112] T. Zhang, R. Barry, K. Knowles, F. Ling, and R. Armstrong, "Distribution of seasonally and perennially frozen ground in the Northern Hemisphere," vol. 2, pp. 1289–1294, 2003.

[113] T. Zhang, B. Tong, and S. Li, "Influence of snow cover on the lower limit of permafrost in Altai Mountains," *Journal of Glaciology and Geocryology*, vol. 7, no. 1, pp. 57–63, 1985.

[114] T. Zhang, "Influence of the seasonal snow cover on the ground thermal regime: An overview," *Reviews of Geophysics*, vol. 43, no. 4, 2005.

[115] T. Zhang, F. E. Nelson, and S. Gruber, "Introduction to special section: Permafrost and seasonally frozen ground under a changing climate," *Journal of Geophysical Research: Earth Surface*, vol. 112, no. F2, 2007.

[116] Y. Zhang, W. Chen, and J. Cihlar, "Transient projections of permafrost distribution in Canada during the 21st century under scenarios of cliamte change," *Journal of Geophysical Research*, no. 18(D22), p. 4695, 2007.

[117] Y. Zhang, S. K. Carey, and W. L. Quinton, "Evaluation of the algorithms and parameterizations for ground thawing and freezing simulation in permafrost regions," *Journal of Geophysical Research: Atmospheres*, vol. 113, no. D17, 2008.

[118] Y. Zhang, S. Wang, A. G. Barr, and T. Black, "Impact of snow cover on soil temperature and its simulation in a boreal aspen forest," *Cold Regions Science and Technology*, vol. 52, no. 3, pp. 355–370, 2008.

[119] Y. Zhang, W. Chen, and D. W. Riseborough, "Transient projections of permafrost distribution in Canada during the 21st century under scenarios of climate change," *Global and Planetary Change*, vol. 60, no. 3, pp. 443–456, 2008.

[120] L. Zhao and D. Gray, "A parametric expression for estimating infiltration into frozen soils," *Hydrological Processes*, vol. 11, no. 13, pp. 1761–1775, 1997.

[121] S. Zoltai, "Southern limit of permafrost features in peat landforms, Manitoba and Saskatchewan," *Geological Association of Canada, Special Paper*, vol. 9, pp. 305–310, 1971.

LIST OF FIGURES

NOMENCLATURE

π_w	Osmotic pressure of a solution [Pa]
α	Contact angle [°]
ΔT	Freezing point depression [K]
γ_{aw}	Surface tension of air-water interface [N m^{-1}]
γ_{iw}	Surface tension of air-water interface [N m^{-1}]
$\hat{r}$	Radius at which occurs the water-ice interface [m]
λ	Brooks and Corey parameter [-]
λ	Thermal conductivity [W m^{-1} T^{-1}]
$\vec{J}_g$	Conduction flux [W m^{-2}]
$\mathcal{E}$	Total energy [J]
$\mathcal{H}$	Sensible heat [W m^{-2}]
μ	Chemical potential [J Kg^{-1}]
μ	Cinematic viscosity of fluid [m^2 s^{-1}]
μ°	Chemical potential of pure water at T_m and p_a [J Kg^{-1}]
μ_i	Chemical potential of ice [J Kg^{-1}]
μ_w	Chemical potential of water [J Kg^{-1}]
ν	Dynamic viscosity of fluid [Pa s]
ν_i	Specific volume of ice [m^3 Kg^{-1}]
ν_w	Specific volume of water [m^3 Kg^{-1}]
ϕ	Soil porosity [-]
Ψ	Suction related to the total water content [m]
ψ	Water suction [m]
ψ_0	Water suction at the inflection point [m]
ψ_a	Air-entry suction [m]
ψ_m	Median suction of $g(\psi)$ [m]
ρ_i	Ice density [Kg m^{-3}]
ρ_w	Water density [Kg m^{-3}]

θ Dimensionless water content [-]

θ_i Dimensionless ice content [-]

θ_r Dimensionless residual water content [-]

θ_s Dimensionless water content at saturation [-]

θ_w Dimensionless liquid water content [-]

$\vec{J}_w$ Heat advected by flowing water [W m^{-2}]

$\underline{E}_T$ Evaporation heat flux [W m^{-2}]

$\underline{J}$ Heat flux due to precipitation [W m^{-2}]

ε Energy per unit volume [W m^{-2}]

$\vec{J}_w$ Water flux [m s^{-1}]

A_{aw} Area of separation surface between water and air [m^2]

A_{iw} Area of separation surface between ice and water [m^2]

c Hydraulic capacity [L^{-1}]

C_a Apparent heat capacity [J m^{-3} K^{-1}]

c_i Specific thermal capacity of ice [J Kg^{-1} K^{-1}]

c_s Specific thermal capacity of soil [J Kg^{-1} K^{-1}]

C_T Total thermal capacity [J m^{-3} K^{-1}]

c_w Specific thermal capacity of water [J Kg^{-1} K^{-1}]

C_{ph} Heat capacity related to the phase change [J m^{-3} K^{-1}]

d Factor describing the soil's structure [m]

E_k Kinetic energy [J]

E_p Potential energy [J]

e_p Potential energy per unit volume [J m^{-3}]

E_T Evapotranspiration [m s^{-1}]

E_T Evapotranspiration [m s^{-1}]

$E_{p,i}$ Potential energy of ice in soil [J]

$e_{p,i}$ Potential energy of ice in soil per unit volume [J m^{-3}]

$E_{p,w}$ Potential energy of water in soil [J]

$e_{p,w}$ Potential energy of water in soil per unit volume [J m^{-3}]

$f(r)$ Pore-size distribution [m^{-1}]

g Gravitational acceleration [m s^{-2}]

$g(\psi)$ Capillary pressure distribution function [m^{-1}]

h Specific enthalpy [J Kg^{-1}]

h Water column height [m]

h_i Specific enthalpy of ice [J Kg^{-1}]

$h_i°$ Specific enthalpy of ice at reference temperature T_{ref} [J Kg^{-1}]

H_s Enthalpy of the soil particles [J]

h_w Specific enthalpy of water [J Kg^{-1}]

$h_w°$ Specific enthalpy of water at reference temperature T_{ref} [J Kg^{-1}]

J Precipitation rate [m s^{-1}]

J Precipitation rate [m s^{-1}]

K Unsaturated hydraulic conductivity [m s^{-1}]

K_r Relative hydraulic conductivity [m s^{-1}]

K_s Hydraulic conductivity at saturation [m s^{-1}]

l Specific latent heat of fusion [J Kg^{-1}]

M Mass [Kg]

m Van Genuchten parameter [-]

M_i Mass of ice [Kg]

M_w Mass of water [Kg]

N Dimensionless factor describing the shape of soil's particles [-]

N Number of pores system [-]

n Van Genuchten parameter [-]

p Pressure [Pa]

p_a Atmosferic pressure [Pa]

p_i Pressure of ice [Pa]

p_w Water pressure [Pa]

r Radius of capillary tube or soil pore [m]

R_n Net radiation [W m^{-2}]

r_{max} Maximum pore radius in the soil [m]

S Entropy [J K^{-1}]

s Specific entropy [J Kg^{-1} K^{-1}]

S_e Effective saturation [-]

S_i Entropy of ice [J K^{-1}]

s_i Specific entropy of ice [J Kg^{-1} K^{-1}]

S_w Entropy of water [J K^{-1}]

s_w Specific entropy of water [J Kg^{-1} K^{-1}]

T Temperature [K]

T^* Temperature at the equilibrium between ice and water [K]

T_i Temperature of ice [K]

T_m Melting point of water [K]

T_w Temperature of water [K]

T_{ref} Reference temperature [K]

u Internal energy per unit volume [J m^{-3}]

U_i Internal energy of ice [J]

u_i Internal energy of ice per unit volume [J m^{-3}]

U_w Internal energy of water [J]

u_w Internal energy of water per unit volume [J m^{-3}]

U_{iw} Internal energy of the ice-water interface [J]

u_{sp} Internal energy of soil particles per unit volume [J m^{-3}]

V Volume [m^3]

V_i Volume of ice in soil [m^3]

V_s Volume of soil [m^3]

V_w Volume of water [m^3]

w_i Weighting factor for each pore system i [-]

x Solute mole fraction in the liquid []